



**Politecnico  
di Torino**

**Politecnico di Torino**

Energy Engineering  
Academic Year 2023/2024  
March 2024

# **Performance analysis of a Microgrid equipped with a Battery Energy Storage System**

Load-Flow and Short-Circuit Calculation on a Microgrid using  
DigSILENT PowerFactory

Supervisor

Prof. Gianfranco CHICCO

Candidate

Matteo MALANDRA



# Abstract

In Scotland, to mitigate the consequences of frequent system anomalies in a remote area of the network, the Distribution Network Operator (DNO) decided to integrate a Battery Energy Storage System (BESS) into the Drynoch primary substation, enabling the downstream network to operate in islanded mode.

The aim of the research is to analyse in depth the behavior of the network once the BESS has been installed. To do this, a load-flow analysis and a short-circuit analysis have been implemented on an approximate network model of the real network. Both analyses have been carried out for different load, generation and operation conditions.

Through the analyses, the main characteristics of the network have been obtained and commented on. In the thesis, in the load-flow analysis, the values of power flows, line loads, voltages in the network nodes and more are discussed, while in the short-circuit analysis the fault currents at the nodes are evaluated.

The analyses have been implemented through PowerFactory, modeling and simulation software for electrical power systems. Within the thesis, all the steps to design the equivalent network and to correctly set the characteristics of each electrical component to properly carry out the analyses are described in detail.



# Table of Contents

List of Figures .....	III
List of Abbreviations .....	V
Introduction .....	1
Part 1: Fundamentals of Microgrid Systems and ESS Technology .....	2
Chapter 1: Microgrid theory .....	2
1.1 The Urgency of Energy Transition .....	2
1.2 Introduction to Microgrids .....	4
1.3 Description of the structure of a Microgrid .....	4
1.4 Operation Modes .....	5
1.5 Technical Challenges .....	6
Chapter 2: ESS .....	7
2.1 Grid-scale Storage Introduction .....	7
2.2 ESS Functionalities in Power Systems .....	8
2.3 ESS Technologies .....	9
2.4 BESS Technology .....	10
Part 2: Network Modeling using DigSILENT PowerFactory .....	13
Chapter 3: Drynoch Primary Substation .....	13
3.1 Introduction to Drynoch Microgrid .....	13
3.2 Primary Substation description .....	15
Chapter 4: Microgrid Modeling .....	16
4.1 Microgrid Modeling Introduction .....	16
4.2 Basic Data Setting of the components .....	17
4.2.1 Busbars .....	17
4.2.2 External Grid .....	18
4.2.3 Transformers .....	19
4.2.4 Earth connections .....	22
4.2.5 BESS .....	25
4.2.6 Neutral Earthing Compensator/Resistor .....	26
4.2.7 Auxiliary Load .....	27
Chapter 5: Distribution System Equivalent Model .....	28
Part 3: Analysis Part .....	34
Chapter 6: Load-Flow Analysis .....	34
6.1 Load-Flow Introduction .....	34

6.2 Load-Flow Mathematical Model.....	36
6.3 Component settings for Load-Flow Analysis.....	39
6.3.1 Terminals.....	39
6.3.2 External Grid .....	40
6.3.4 Transformers .....	41
6.3.5 Loads.....	44
6.3.6 Wind Turbine .....	46
6.3.7 Virtual Power Plant (VVP) .....	47
6.3.8 Station Controller.....	48
6.3.9 BESS .....	49
6.4 Load-Flow Command Settings .....	51
6.5 Load-Flow Analysis Results .....	53
Chapter 7: Short-Circuit Analysis .....	59
7.1 Short-Circuit Analysis Theory.....	59
7.2 Component Setting for Short-Circuit Analysis .....	63
7.2.1 External Grid .....	63
7.2.2 Transformers .....	64
7.2.3 Lines.....	65
7.2.4 BESS .....	66
7.2.5 Wind Turbine .....	67
7.3 Short-Circuit Command Settings.....	69
7.4 Short-Circuit Analysis Results .....	71
Conclusions.....	78
Bibliography.....	81
Ringraziamenti.....	83

# List of Figures

FIG. 1.1 ATMOSPHERIC CARBON DIOXIDE TREND.....	2
FIG. 1.2 CLEAN ENERGY INVESTMENT AND REDUCTION IN FOSSIL FUEL IMPORT BILLS IN DEVELOPING ECONOMIES IN ASIA IN THE NZE SCENARIO RELATIVE TO THE STEPS.....	3
FIG. 2.1 ANNUAL GRID-SCALE BATTERY STORAGE ADDITIONS, 2017-2022. ....	7
FIG. 2.2 DIFFERENT TYPE OF FUEL CELLS. ....	9
FIG 2.3 DISCHARGE TIME AND POWER RATING OF ESS. ....	10
FIG. 2.4 COST OF LITHIUM CARBONATE, CHINESE YUAN/TON. ....	11
FIG 3.1 LOCATION OF DRYNOCH IN THE ISLAND OF SKYE. ....	14
FIG. 3.2 DRYNOCH LOAD DATA. ....	14
FIG. 3.3 DRYNOCH PRIMARY SUBSTATION MODEL. ....	15
FIG. 4.1 COMPONENT DATA HIERARCHY IN POWERFACTORY. ....	16
FIG. 4.2 TERMINAL BASIC DATA. ....	17
FIG. 4.3, 4.4 EXTERNAL GRID BASIC DATA. ....	18
FIG. 4.5 HIGH VOLTAGE TRANSFORMER TYPE OBJECT BASIC DATA. ....	19
FIG. 4.6 HIGH VOLTAGE TRANSFORMER ELEMENT OBJECT BASIC DATA, GENERAL PAGE. ....	20
FIG. 4.7 HIGH VOLTAGE TRANSFORMER ELEMENT OBJECT BASIC DATA, GROUNDING/NEUTRAL CONDUCTOR. ....	20
FIG. 4.8 BESS TRANSFORMER TYPE OBJECT BASIC DATA. ....	21
FIG. 4.9 BESS TRANSFORMER ELEMENT OBJECT BASIC DATA, GENERAL PAGE. ....	21
FIG. 4.10 BESS TRANSFORMER ELEMENT OBJECT BASIC DATA, GROUNDING/NEUTRAL CONDUCTOR. ....	22
FIG 4.11 BESS TRANSFORMER EARTHING CONNECTION. ....	22
FIG. 4.12 HIGH VOLTAGE TRANSFORMER EARTHING CONNECTION CIRCUIT BREAKER, BASIC DATA. ....	23
FIG. 4.13 HIGH VOLTAGE TRANSFORMER SERIES RLC FILTER, BASIC DATA. ....	23
FIG. 4.14 HIGH VOLTAGE TRANSFORMER GROUNDING SWITCH, BASIC DATA. ....	24
FIG. 4.15 BESS TRANSFORMER EARTHING CONNECTION CIRCUIT BREAKER, BASIC DATA. ....	24
FIG. 4.16 BESS TRANSFORMER SERIES RLC FILTER, BASIC DATA. ....	25
FIG. 4.17 BESS TRANSFORMER GROUNDING SWITCH, BASIC DATA. ....	25
FIG. 4.18 BESS BASIC DATA, GENERAL PAGE. ....	26
FIG. 4.19, 4.20 NEC/NER BASIC DATA, GENERAL AND GROUNDING/NEUTRAL CONDUCTOR PAGE. ....	26
FIG. 4.21 AUXILIARY LOAD BASIC DATA. ....	27
FIG 5.1 LUMPED PARAMETER MODEL FOR A SINGLE-PHASE AC LINE. ....	28
FIG. 5.2 LOAD TRANSFORMER TYPE OBJECT, BASIC DATA. ....	30
FIG. 5.3 WIND GENERATION TRANSFORMER TYPE OBJECT, BASIC DATA. ....	31
FIG. 5.4 EQUIVALENT DISTRIBUTION NETWORK MODEL. ....	31
FIG. 6.1 TERMINAL LOAD FLOW DATA. ....	39
FIG. 6.2 EXTERNAL GRID LOAD FLOW DATA, GENERAL PAGE. ....	40
FIG. 6.3 EXTERNAL GRID LOAD FLOW DATA, ADVANCED PAGE. ....	41
FIG. 6.4 EXTERNAL GRID LOAD FLOW DATA, AUTOMATIC DISPATCH. ....	41
FIG. 6.5, 6.6 HIGH VOLTAGE TRANSFORMER TYPE OBJECT LOAD FLOW DATA, GENERAL AND TAP CHANGER PAGE. ....	42
FIG. 6.7, 6.8 HIGH VOLTAGE TRANSFORMER ELEMENT OBJECT LOAD FLOW DATA, GENERAL AND CONTROLLER, TAP CHANGER 1 PAGE. ....	43
FIG. 6.9, 6.10 BESS TRANSFORMER AND LOAD TRANSFORMER TYPE OBJECT LOAD FLOW DATA, GENERAL PAGE. ....	43
FIG. 6.11 WIND GENERATION TRANSFORMER TYPE OBJECT LOAD FLOW DATA, GENERAL PAGE. ....	44
FIG. 6.12 DRYNOCH LOAD DATA. ....	44
FIG. 6.13 LOAD FLOW DATA OF LOAD 2B, GENERAL PAGE. ....	45
FIG. 6.14 WIND GENERATION LOAD FLOW DATA, GENERAL PAGE. ....	46

FIG. 6.15 WIND GENERATION LOAD FLOW DATA, OPERATIONAL PAGE. ....	47
FIG 6.16 STATION CONTROLLER BASIC DATA. ....	48
FIG 6.17 STATION CONTROLLER LOAD FLOW DATA, GENERAL PAGE. ....	48
FIG 6.18 BESS LOAD FLOW DATA, GENERAL PAGE. ....	49
FIG. 6.19 BESS LOAD FLOW DATA, OPERATIONAL LIMITS PAGE. ....	50
FIG. 6.20 LOAD FLOW COMMAND, BASIC DATA PAGE. ....	51
FIG. 6.21 LOAD FLOW COMMAND, ACTIVE POWER CONTROL PAGE. ....	52
FIG. 6.22 LOAD FLOW COMMAND, CALCULATION SETTINGS PAGE. ....	52
FIG. 6.23 DRYNOCH PRIMARY SUBSTATION MODEL. ....	53
FIG. 6.24 EQUIVALENT DISTRIBUTION NETWORK MODEL. ....	53
FIG. 7.1 SHORT-CIRCUIT TRANSIENT. ....	59
FIG 7.2 IEC SUPERIMPOSITION METHOD. ....	60
FIG. 7.3 VOLTAGE CORRECTION FACTORS. ....	61
FIG. 7.4 SUPERIMPOSITION COMPLETE METHOD. ....	61
FIG. 7.5 EXTERNAL GRID COMPLETE METHOD DATA. ....	63
FIG. 7.6 LINE TYPE COMPLETE METHOD DATA. ....	65
FIG. 7.7 BESS SC CURRENT PIECEWISE FUNCTION. ....	66
FIG 7.8 BESS COMPLETE METHOD PAGE. ....	67
FIG 7.9 WIND TURBINE COMPLETE METHOD PAGE. ....	68
FIG. 7.10 BASIC OPTIONS, SHORT CIRCUIT COMMAND. ....	69
FIG. 7.11 ADVANCED OPTIONS, SHORT CIRCUIT COMMAND. ....	70
FIG. 7.12 DRYNOCH PRIMARY SUBSTATION MODEL. ....	71
FIG. 7.13 EQUIVALENT DISTRIBUTION NETWORK MODEL. ....	71



# List of Abbreviations

<b>ABBREVIATION</b>	<b>DEFINITION</b>
<b>DNO</b>	Distribution System Operator
<b>BESS</b>	Battery Energy Storage System
<b>SW</b>	Software
<b>ESS</b>	Energy Storage System
<b>RES</b>	Renewable Energy Source
<b>DER</b>	Distributed Energy Source
<b>MEG</b>	Microgrid Exchange Group
<b>RTU</b>	Remote Terminal Unit
<b>SCADA</b>	Supervisory Control and Data Acquisition
<b>EMS</b>	Energy Management System
<b>IEA</b>	International Energy Agency
<b>SSEN</b>	Scottish and Southern Electricity Network
<b>TSO</b>	Transmission System Operator
<b>IGB</b>	Inverter Based Generators
<b>SC</b>	Supercapacitor
<b>SMES</b>	Superconducting magnetic energy storage systems
<b>WG</b>	Wind Generation
<b>VVP</b>	Virtual Power Plant
<b>SOC</b>	State Of Charge



# Introduction

On the Isle of Skye, Scotland, the Distribution Network Operator (DNO) has decided to install an Energy Storage System (ESS) based on lithium-ion battery technology in the Drynoch primary substation. This decision derives from the need to make energy dispatching safer and more flexible, in a rural location that is difficult to access and for which a possible expansion would have been economically prohibitive.

By installing the Battery Energy Storage System (BESS), the downstream network is enabled to operate in islanded mode. In other words, in the event of a fault occurring in the network upstream the substation, the distribution network under analysis would operate individually, internally satisfying the energy demand through the BESS and the distributed generation present in the network.

The aim of the thesis is to analyse the performance of the network, whether connected to the national grid or not, through the power system simulation software called DigSilent PowerFactory. Two different analyses have been carried out with the software: load-flow analysis and short-circuit analysis.

All the network data downstream the Drynoch primary substation and the data of the storage system in the design phase were made available by Loccioni, an Italian specialist system integrator and battery storage system provider, partner of Oiko Energy, an engineering firm for the design of systems in the renewables field where I personally work and am carrying out the thesis. Loccioni was directly commissioned by the DNO and other partners for the design and installation of the storage system.

The study is divided into three main parts. In the first part, the concept of microgrid is introduced, exposing all its characteristics and their importance for the energy transition, as well as the main storage technologies on the market, with a greater focus on lithium-ion batteries, the technology used in the network under study.

In the second part, both the distribution network and the PowerFactory software are exposed. Accordingly, the step-by-step process for modeling the network in the Software (SW) is shown.

The third part concerns the setting up of the analysis and the presentation and discussion of the results.

# Part 1: Fundamentals of Microgrid Systems and ESS Technology

The purpose of this first part of the report is to provide a basic idea of the concepts regarding the microgrids equipped with ESS. Therefore, the importance of microgrids for the energy transition, its characteristics, benefits and critical issues, operating methods and others crucial topics are presented. The technologies used for electrical storage are analysed, with a particular focus on BESS, since the microgrid that is analysed is equipped with a lithium-ion BESS.

## Chapter 1: Microgrid theory

### 1.1 The Urgency of Energy Transition.

In the contemporary era, one of the most difficult challenges that the world must face is global warming. Human activities have caused a constant increase in greenhouse gases within the atmosphere, with a consequent growth of medium temperatures around the world.

Fig. 1.1 shows the growth in carbon dioxide concentration in the last decades since 1960 in the atmosphere:

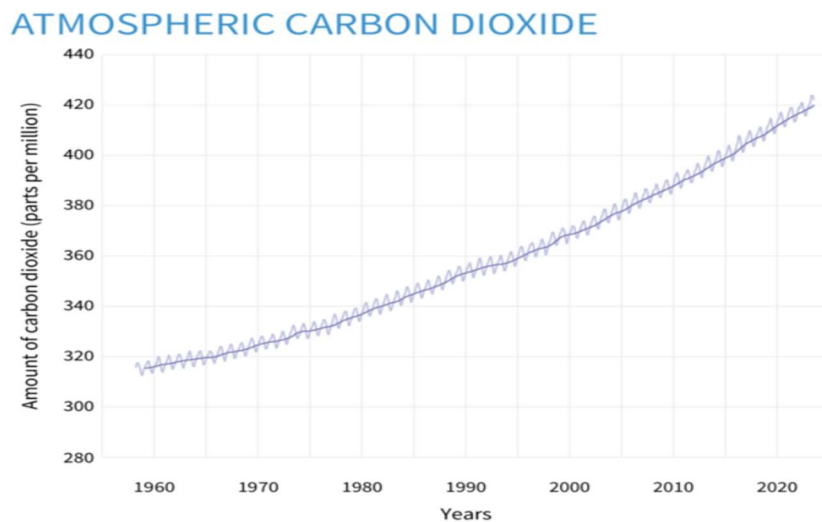
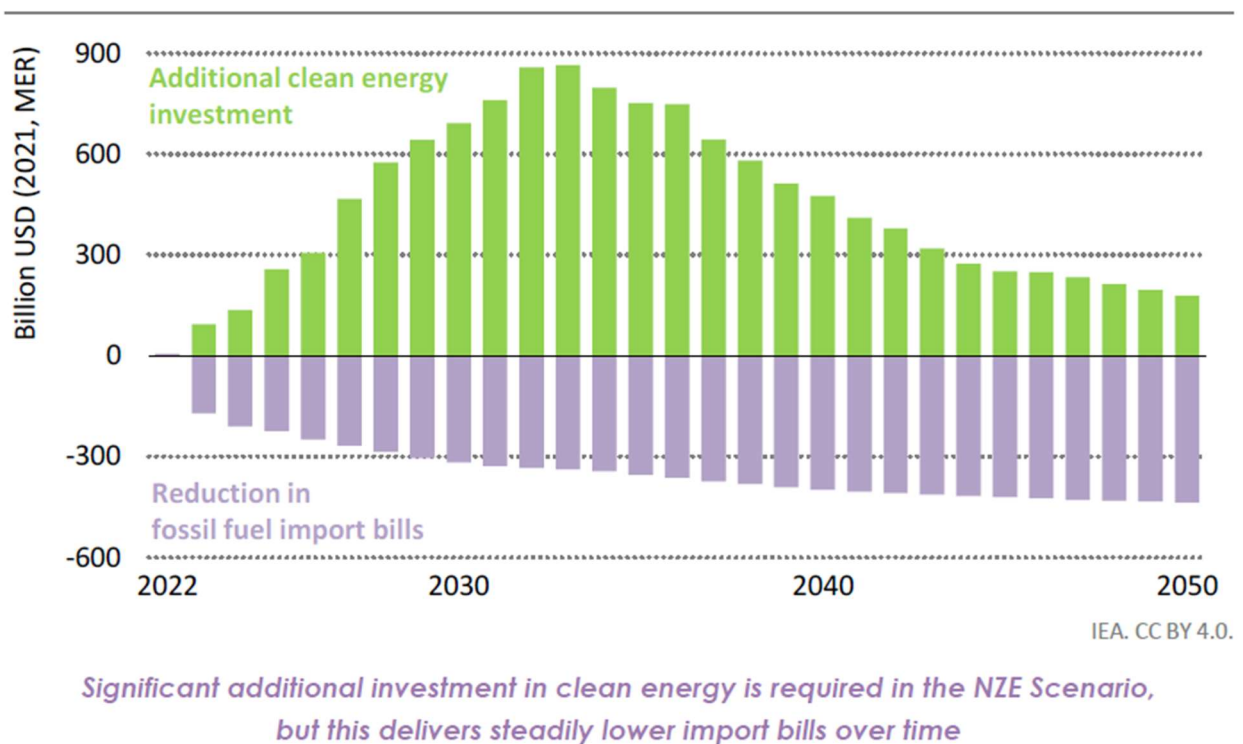


Fig. 1.1 Atmospheric Carbon Dioxide Trend. [1]

Given the monotonous trend, each year is destined to break the previous record. The medium amount of CO<sub>2</sub> around the globe was almost 420 parts per million in 2022. This concentration has doubled compared to pre-industrial levels [1].

The only solution to solve this issue is to perform a global energy transition, reducing the dependency on fossil fuels, which are the primary cause to global warming. In Europe, the 77% global greenhouse emissions are attributed to the energy sector [2].

To address climate change issue, there is an urgent need for cooperation among all nations worldwide, and a greater economic-political effort than that made in previous years. Just to provide an idea, Fig. 1.2 is shown: it illustrates the additional clean energy investments and the reduction in fossil fuel import bills that need to be done in the following years by developing countries to reach the net zero scenario:



Note: NZE = Net Zero Emissions by 2050 Scenario; STEPS = Stated Policies Scenario; MER = market exchange rate.

Fig. 1.2 Clean energy investment and reduction in fossil fuel import bills in developing economies in Asia in the NZE Scenario relative to the STEPS. [3]

Continuing the abuse of finite sources, such as coal, oil, and fossil natural gas, would bring without any doubts to irreversible environmental repercussions that will have a negative impact on the quality of life for all of humanity.

## 1.2 Introduction to Microgrids

For a few years now, many countries have been wanting to move from a centralized energy generation to a distributed one. This is for several reasons. Distributed generation can be much more efficient than centralized generation, given the significantly shorter distance to serve the demand. Moreover, being able to accommodate small-scale generation plants in the distribution system means being able to integrate Renewable Energy Sources (RES) within the energy share, decreasing fossil fuel dependency. Although the large-scale integration of Distributed Energy Resources (DERs) is not easy to carry out, also because the cost per unit of power of DERs is greater than the same costs relating to centralized generation due to the effects of the economy of scale, for the reasons explained it is fundamental to speed up the energy transition.

As defined by the Microgrid Exchange Group (MEG), “A microgrid is a group of interconnected loads and distributed energy resources within clearly defined electrical boundaries that acts as a single controllable entity with respect to the grid. A microgrid can connect and disconnect from the grid to enable it to operate in both grid-connected or island-mode.” [4].

## 1.3 Description of the structure of a Microgrid

As mentioned, a microgrid is a portion of the network equipped with distributed generation elements and electrical loads. It is generally connected to the national grid, but which can self-sustain its own electricity demand in the event of a fault in the main network.

To achieve the objective of satisfying demand efficiently in economic and energy terms while preserving the safety of the system, the microgrid is equipped with complicated control, monitoring safety and advanced metering systems.

RTUs (Remote Terminal Units) provide measurements and states of the network to the SCADA (Supervisory Control And Data Acquisition), which is able to store and analyse the information received. Depending on the state of the network, SCADA can take actions, such as maintaining a certain power factor of a generator, reporting an alarm, controlling a circuit breaker and more. Moreover, a microgrid must be equipped with an Energy Management System (EMS), which considers the state estimation and the security state of the network, together with economic or market data, to evaluate the best dispatching strategy.

Unlike traditional networks, the direction of power flows is not unique: for this reason, a measurement system is needed to be aware of the flow exchanges between the different areas of the network [5] [6].

## 1.4 Operation Modes

A microgrid is capable to work in two fundamental modes, grid connected mode and islanded mode. The choice of mode of operation will depend on several factors, such as the grid connectivity, the energy source availability, the presence of anomalies and others:

- **Grid-Connected Mode**

In this configuration, the microgrid works in parallel with the main electricity network.

The energy generated can be transferred to the main network grid when the microgrid produces more energy than it needs. In contrast, if the energy sources present in the microgrid are not sufficient to fulfill the local electrical load, the mismatch between energy produced and requested will be filled by energy injection from the main grid. In general, the microgrid and the main network communicate to optimize the dispatching strategy, based on the technical-economic constraints.

An important role played by the microgrid is to enhance grid stability; indeed, it can adjust its generation output in response to grid frequency and voltage fluctuations.

The exploitation of local energy generation, due to the shorter distance between the energy sources and local loads, causes a considerable decrease of transmission losses.

- **Islanded Mode**

In this scenario, the microgrid operates independently of the main grid. The network is supplied by the penetration of DERs and by ESS.

This mode can be the default one or can be activated in the event of a failure of the main network. While operating in this mode, the microgrid must guarantee the quality of delivery according to regulations.

In this mode of operation, the EMS optimizes the use of the limited generation within the confines of the microgrid and communicates with the external grid for reconnection [7].

## 1.5 Technical Challenges

Although moving from a centralized to distributed generation model offers many advantages to the society, the transformation path of the electricity grid is a difficult task to accomplish. This paragraph will focus in detail on the criticalities implementing such technology:

1. **Operation:** As microgrids have the capability to work in different modes of operation, considerable mismatches between power generation and demand can arise, resulting in notable challenges related to frequency and voltage control.
2. **Compatibility:** A microgrid is composed of various generation units, such as PV panels, wind turbines, energy storage systems, CHP units and more. Each component exhibits distinct characteristics including power generation capacity, startup and shutdown times, inertia, operational costs, charging/discharging rates, control mechanisms, and communication constraints. Such differences between units make optimal dispatching of resources complicated.
3. **Protection:** The most challenging technical concern related to the integration of distributed generators into microgrids revolves around system protection. While for traditional power systems the operating mode of the protections is more univocal, in the case of microgrids the protections must be able to protect the system and the loads in all the possible configurations that the microgrid can assume.
4. **Integration of RES:** The uncertainty and intermittent nature of RES pose substantial challenges to their seamless integration into the power grid. The output power from these resources can exhibit significant and frequent fluctuations, thereby introducing instability to microgrids.
5. **Regulation:** An important challenge is to implement regulation on microgrids. Through standardization and regulation, it is possible to facilitate the transition from a centralized power system model to a more distributed model. Defining the regulations is not easy, given that there are a series of technical-economic constraints to respect [8].



# Chapter 2: ESS

## 2.1 Grid-scale Storage Introduction

Grid-scale storage is a device connected to the network able to store energy and deliver it in a more convenient moment. Its integration to microgrid will be fundamental for the proper integration of renewable resources such as wind and solar power plant, and for making progress in the energy transition. Fig. 2.1 made by IEA (International Energy Agency) shows the global annual grid-scale battery storage additions in GW from 2017 up to 2022:

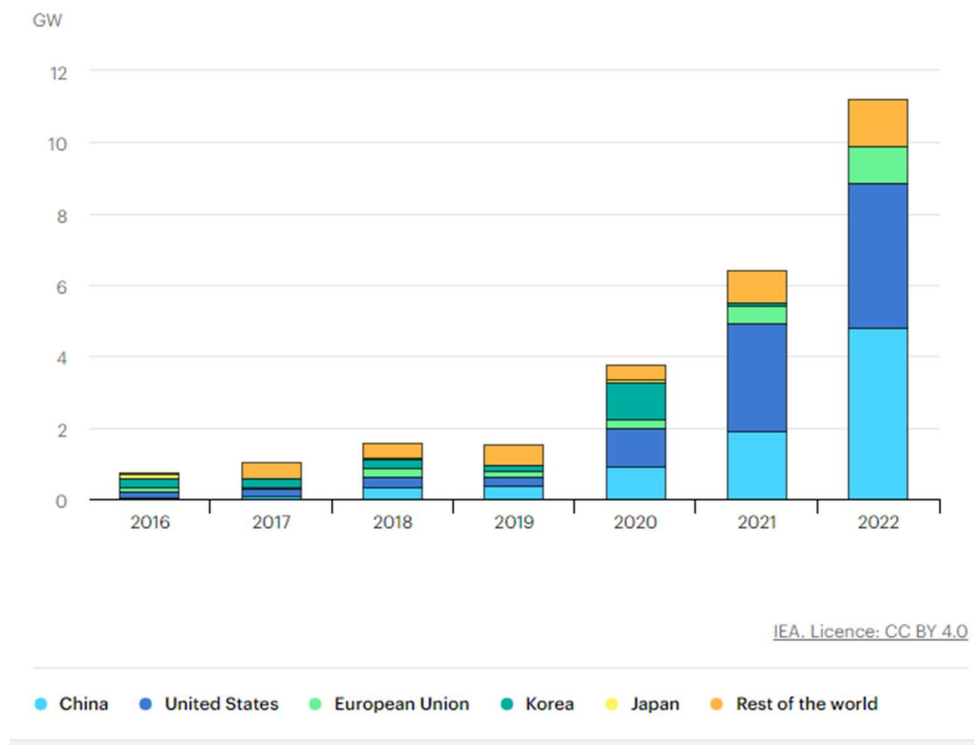


Fig. 2.1 Annual grid-scale battery storage additions, 2017-2022. [9]

The growth in investment in technology by some world powers is evident from the graph. Quoting the IEA: “China led the market in grid-scale battery storage additions in 2022, with annual installations approaching 5 GW. This was followed closely by the United States, which commissioned 4 GW over the course of the year. The Inflation Reduction Act, passed in August 2022, includes an investment tax credit for stand-alone storage, promising to further boost deployments in the future.” [10].

This chapter explains the main energy storage technologies used in microgrids, as well as their main functions.

## 2.2 ESS Functionalities in Power Systems

The functions of ESS in power systems are not limited to just provide an electricity storage service to the grid and to absorb/inject energy. They are also useful for:

- **Power quality:** Thanks to the diffusion of sensitive electrical equipment, TSOs and DSOs can cooperate to ensure good voltage and frequency stability, trying also to minimize electrical disturbances as much as possible. ESS can be useful to mitigate short-term loss of power and power fluctuations.
- **ESS integration with DERs:** Going forward through the energy transition, replacing the fossil energy source with greener solution, the modern energy resources are going to be more and more difficult to control than the conventional ones. Inverter Based Generators (IBGs), such as wind energy and photovoltaics, don't ensure the continuity of energy production. For this reason, ESS are essential for the proper integration of RES in the distribution network, allowing the transition towards an eco-friendlier electrical network.
- **Voltage support:** The system voltage must be controlled to keep it within an upper and a lower limit. Usually, it is done by varying the transformation ratio of the transformer and/or reactive power flows. In distribution network, where the ratio X/R is lower, the voltage is also regulated by active power injection and absorption. In this case, ESS can be very useful, since it is able to inject both reactive and active power.
- **Energy time shifting:** The ESS can be used to store electricity when the demand is low. This electricity will be discharged during peak demand periods. It considerably increases the efficiency of energy utilization.
- **End use energy management:** In times where energy demand and energy costs are high, DSOs often offer compensations to customers who accept a reduction or total cut in their energy consumption. The disposition of this technology by the customers makes them much more inclined to accept such offers, given the greater flexibility of consumption.
- **Load Following:** This service consists of matching small and frequent variation of load demand. ESS technologies such as ion lithium batteries and supercapacitors are suitable to cover this service, because of their high efficiency at partial load and their quick time response.
- **Capacity of distribution circuit:** With the increase of DERs, ESS can be useful to defer distribution network repowering [6], [11], [12].

## 2.3 ESS Technologies

Below, some technologies that can be used as energy storage systems within the electricity grid are briefly described. The microgrid that will be analysed in the thesis is equipped with a lithium-ion battery storage system. For this reason, this technology will not appear in the list, but a separate paragraph will be dedicated to it:

1. **Flywheel:** It is a rotating wheel mounted on a shaft that stores energy in rotational form. By slowing down or increasing its rotation, it is capable of respectively releasing and accumulating energy [12]. High-speed flywheels usually work in a vacuum to minimize friction losses as much as possible [11].
2. **Fuel Cell:** A fuel cell is an electrochemical cell that transforms the chemical energy of a fuel into electricity. The fuel, typically hydrogen or methane, is usually oxidized by air or pure oxygen. There are several types of fuel cells, and they differ from operating temperature, the fuel used, the electrolyte and more [13]. Figure 2.2 illustrates some examples:

Type	Electrolyte	Operating temperature	Maximum output power reported
Polymer Electrolyte Membrane (PEM)	Organic polymer	80 °C	250 kW
Alkaline Fuel Cells (AFC)	Potassium hydroxide	150–200 °C	12 kW
Phosphoric Acid Fuel Cell (PAFC)	Phosphoric acid	150–200 °C	250 kW
Molten Carbonate Fuel Cells (MCFC)	Potassium, sodium or lithium carbonate	650 °C	2 MW
Solid Oxide Fuel Cells (SOFC)	Ceramic materials	1000 °C	100 kW

Fig. 2.2 Different type of Fuel Cells. [11]

3. **Supercapacitor (SC):** A supercapacitor is a capacitor with high capacity, able to store and deliver a massive amount of power in a small time. For this feature, they play a key role for grid stability. [6], [12].
4. **Superconducting magnetic energy storage systems (SMES):** the energy is stored in a superconductive coil in magnetic form. This type of coil has the advantage of having negligible resistive losses, therefore the energy stored in it is conserved. The coil is maintained at cryogenic temperature to minimize resistances [11].

The choice of type of ESS strongly depends on the grid needs. While certain technologies can discharge high power in a short time and offer a high number of cycles over time, others are more suitable for introducing a high quantity of energy, are characterized by longer discharge times and a lower number of cycles over time. Just as an example, supercapacitors, which feature high power density, are perfect for providing frequency quality services. BESS on the other hand, having a higher capacity, are more suitable for powering loads.

Figure 2.3 shows a comparison between technologies according to power rating and discharge time. The color associated in the graph by each technology depends on its conversion efficiency.

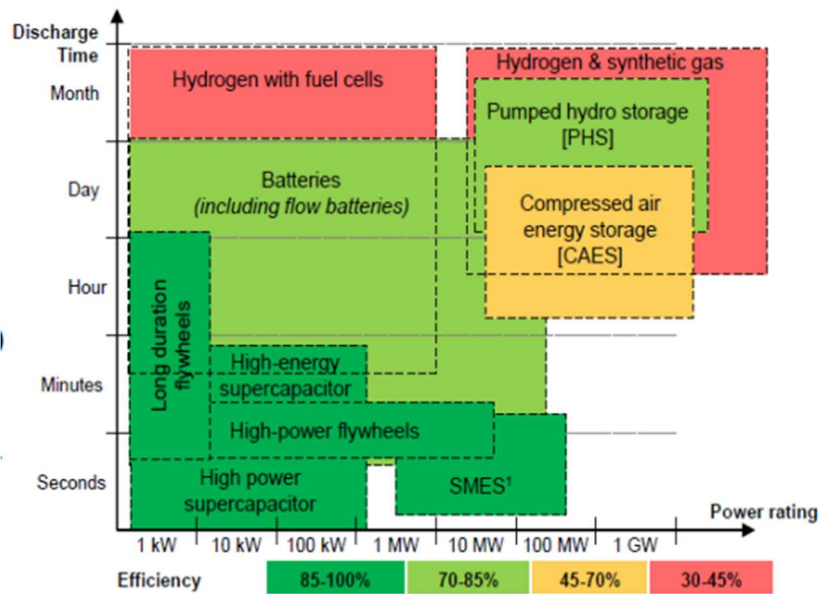


Fig 2.3 Discharge Time and Power Rating of ESS. [6]

## 2.4 BESS Technology

A BESS is a storage system that uses batteries to store and inject power. This technology is used in various sectors, such as in electricity distribution, in the automotive sector and in the home automation sector. In power systems, BESS are connected to the grid system through inverters, which convert electrical energy from direct to alternating. They are equipped with control systems, sensors, and various auxiliary components that guarantee its correct functioning.

BESS can cover many functions. It can be used as a backup generator, for those activities that require guaranteed energy. Furthermore, by storing energy in periods where costs are relatively low, they can feed energy into the grid during periods of peak demand. The last service described fully explains the usefulness of technology in energy dispatching, being able to offer flexibility to dispatching and the possibility of compressing demand in a cost-effective way even in the most critical periods [14].

The dimensions of the storage systems and the type of battery chemistries define the main characteristics of the BESS. Below, the most important characteristics are mentioned [15]:

- Rated Power Capacity
- Rated Energy Storage
- Storage Duration
- Depth of Discharge (DoD)
- Discharge Rate
- Round-trip Efficiency
- Response Time
- Cycle life / lifetime

Among the most used battery types, there are:

- **Lithium-ion (Li-Ion):** it is the most used battery in energy storage applications. Depending on the type of cathode used, Lithium iron phosphate (LFP) and lithium nickel manganese cobalt oxide (NMC) can be distinguished. Li-Ion batteries are light and characterized by high capacity and energy density. They offer a long lifespan and maintenance costs are minimal. Despite this, they are flammable and cannot operate at high temperatures.
- **Lead-Acid (PbA):** Although they are characterized by lower energy and a higher density discharge time than Li-Ion batteries, Lead-Acid batteries are widely used in the automotive sector and as uninterruptible power supply. They are widely available in the market at low prices and can operate over a wide temperature range.
- **Zinc Bromine:** This type of battery was designed as a replacement for the most popular Lithium-ion batteries on the market. They are used both on a domestic and grid scale. Although performance is lower than lithium-ion batteries, the aqueous nature of the electrolyte makes them less susceptible to temperature problems.
- **Sodium-Sulphur (Na-S):** This technology is characterized by a long lifespan and high energy density. Due to the high operation temperature, they are not suitable for domestic use. Moreover, the presence of sodium makes them susceptible to explosions [15].

Large scale batteries are becoming very popular in the current years. Even if the cost of the technology is decreasing, to continue along this trend will depend on critical mineral prices, fundamental to produce clean energy technology [16]. Fig. 2.4 shows the trend of the cost of lithium carbonate in the recent years:

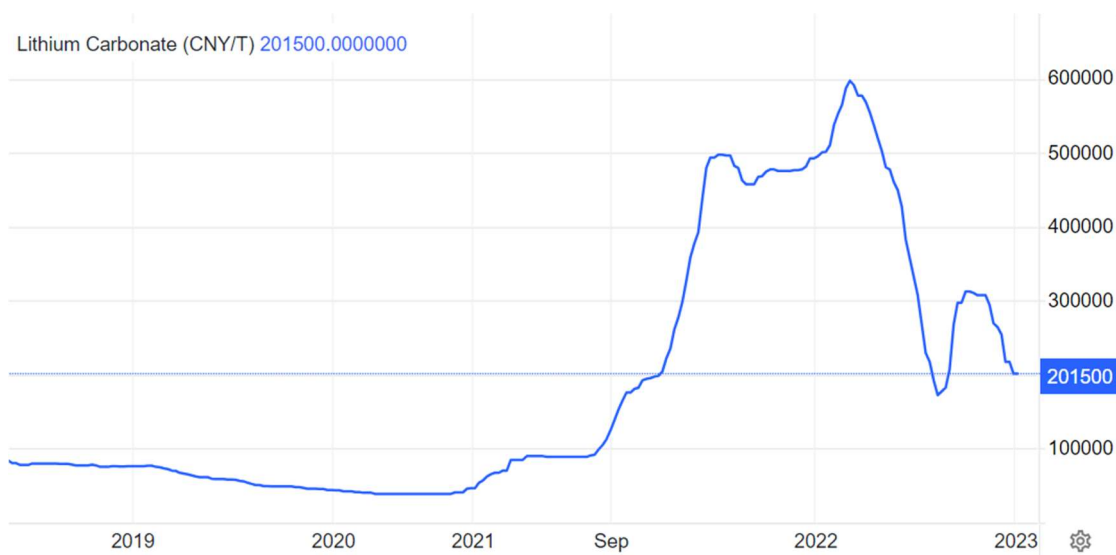


Fig. 2.4 Cost of Lithium Carbonate, Chinese Yuan/Ton. [17]



# Part 2: Network Modeling using DIgSILENT PowerFactory

## Chapter 3: Drynoch Primary Substation

### 3.1 Introduction to Drynoch Microgrid

The microgrid under study is part of a project delivered by three partners: SSEN, E.ON and Costain. SSEN (Scottish and Southern Electricity Networks) are the distribution network operator, E.ON are an energy solutions provider, while Costain are a management consultancy acting as a program manager [18].

The objective of the project is to provide a novel flexibility service based on market principles, specifically designed for use by DNO to enhance the resilience of power grids in isolated or rural regions that are prone to experiencing power outages. This innovative service incorporates a BESS in the network. The primary goal is to ensure the continuous supply of electricity to customers in the event of a network fault, thereby addressing vulnerabilities in remote areas susceptible to power outages [19].

It is important to mention that the BESS integration is still in the planning phase. For some years now, the partners have joined forces to understand in principle what the technical requirements of the work should be, based on in-depth market analyses, software simulations of the performance of the network equipped with BESS, considering the future expansions planned to accommodate increased demand. Based on the main technical specifications of the system collected, Loccioni, an Italian specialist system integrator and battery storage system provider, was entrusted with the design refinement and construction of the system.

The substation chosen for the installation of the BESS system is situated in Drynoch, which is located near the south-east tip of Loch Harport on the west coast of Skye in the Highlands of Scotland [19].

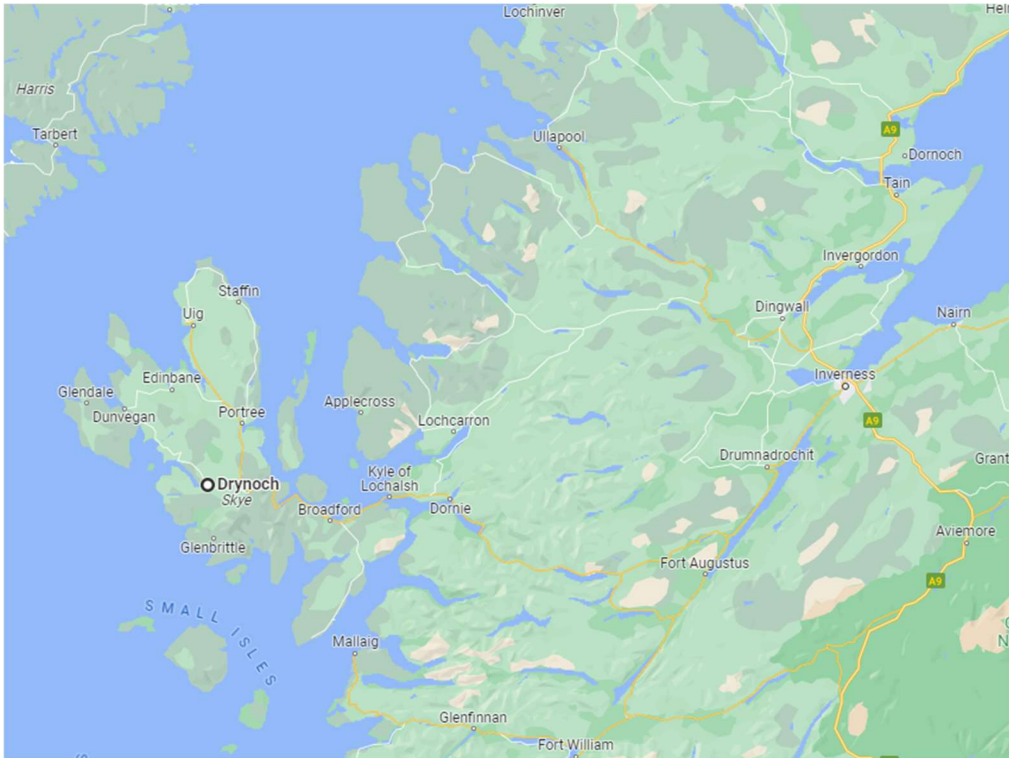


Fig 3.1 Location of Drynoch in the Island of Skye [19].

The substation supplies power to around 1000 customers connected to the electrical grid. It is a 33 kV to 11 kV primary substation. The peak demand recorded from the year 2015 to year 2019 is equal to 1,78 MVA. The nominal power of the embedded generation connected to the 11 kV network was of 0,73 MVA. Fig. 3.2 shows the overall demand trend within the years mentioned [19].

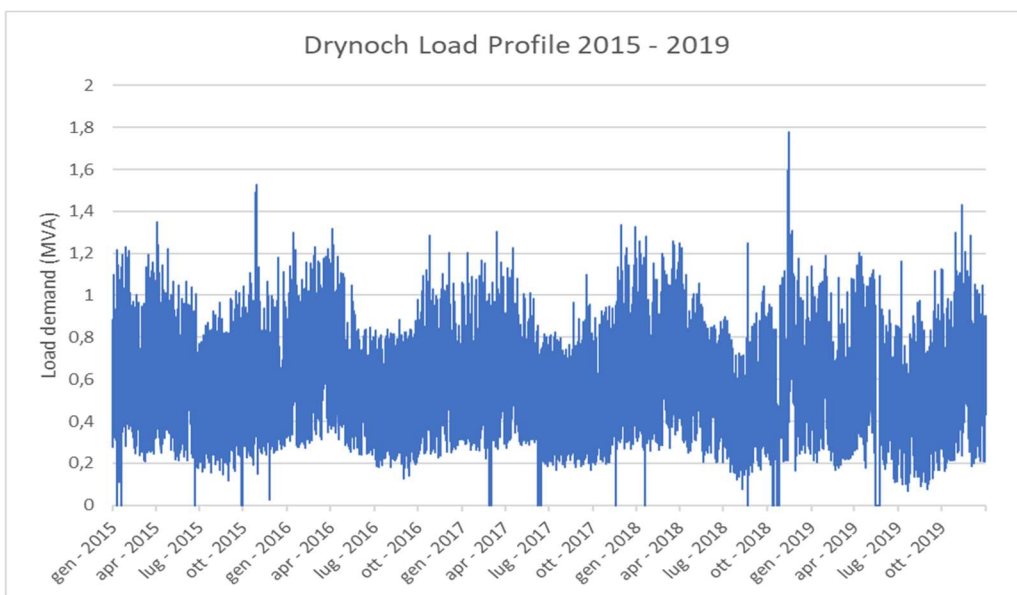


Fig. 3.2 Drynoch Load Data [19].



## 3.2 Primary Substation description

Drynoch primary substation is connected on a single radial feeder at 33 kV from the Grid. A two-windings 2.5 MVA Yyn0 33 kV /11 kV oil filled transformer allows the connections. The 11 kV winding is equipped with an earthing connection. Downstream the transformer, a circuit breaker is installed before the 11 kV busbar. Two feeders, equipped in turn with one circuit breaker each, are connected to the 11 kV busbar.

Regarding the BESS side, the ion lithium batteries and their auxiliary system are connected to the 11 kV busbar by means of a two-winding 3 MVA 11 kV / 1 kV transformer. In the latter, an earthing connection is linked to the primary windings. Finally, it is important to point out the presence of two other circuit breakers: one between the batteries and the LV windings of the transformer and another between the high voltage windings and the 11 kV busbar [19].

To make the description clearer, the preview of the model created on PowerFactory is shown in Fig. 3.3.

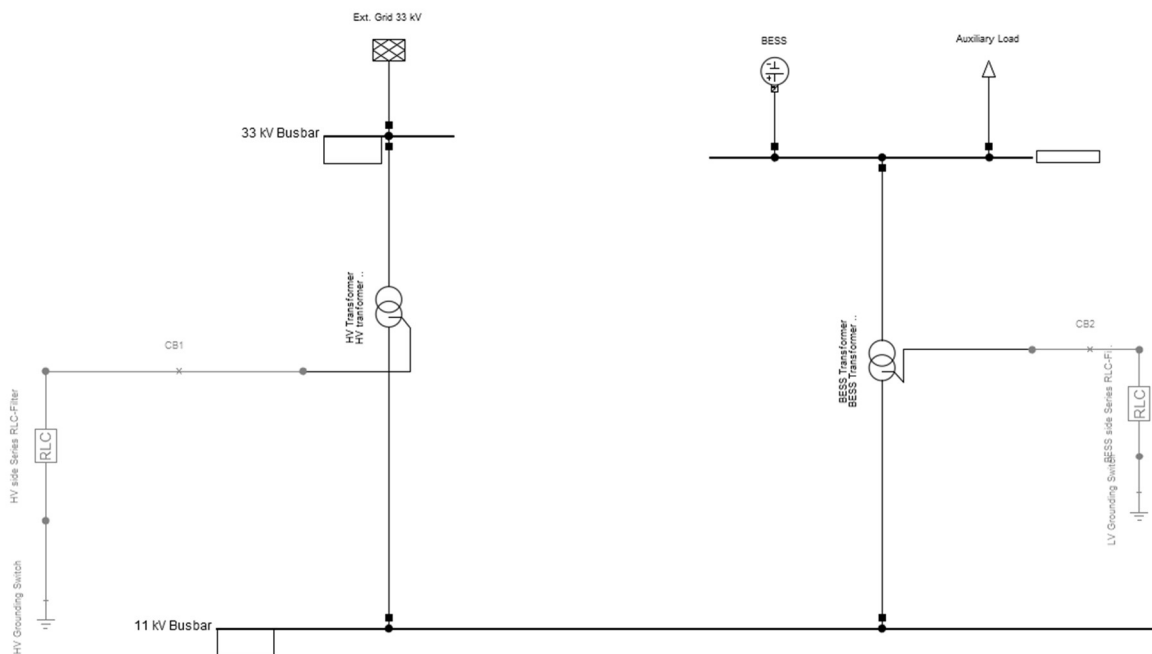


Fig. 3.3 Drynoch primary substation model.

Note that in this picture, the two feeders connected to the 11 kV busbar have not been represented.

# Chapter 4: Microgrid Modeling

## 4.1 Microgrid Modeling Introduction

As previously mentioned, the fundamental aim of this study is to evaluate, through the development of various analyses, the performance and therefore the quality of service within a microgrid, which can work in parallel with the main grid or in islanded mode.

The software named PowerFactory was used to perform the analyses. PowerFactory is a software developed by DigSilent that allows to simulate the behavior of power system networks and carry out different types of calculations [20].

To give an idea of the software's functionality, PowerFactory allows to carry out short-circuit analyses to size the protections within the system, to optimize the energy transmission process by minimizing losses within the network, to evaluate the stationary or transient performances of the network such as the loading status of the components to evaluate any reinforcement of the network. By means of PowerFactory, studies can be carried out on the quality of service in terms of frequency and voltage. It is therefore a useful tool both for evaluating functioning networks and for predicting the behavior of networks in the design phase.

All the steps to model the network are described in the following paragraphs. Fig. 4.1 is shown only to clarify the data storage relating to the components of the network within the software.

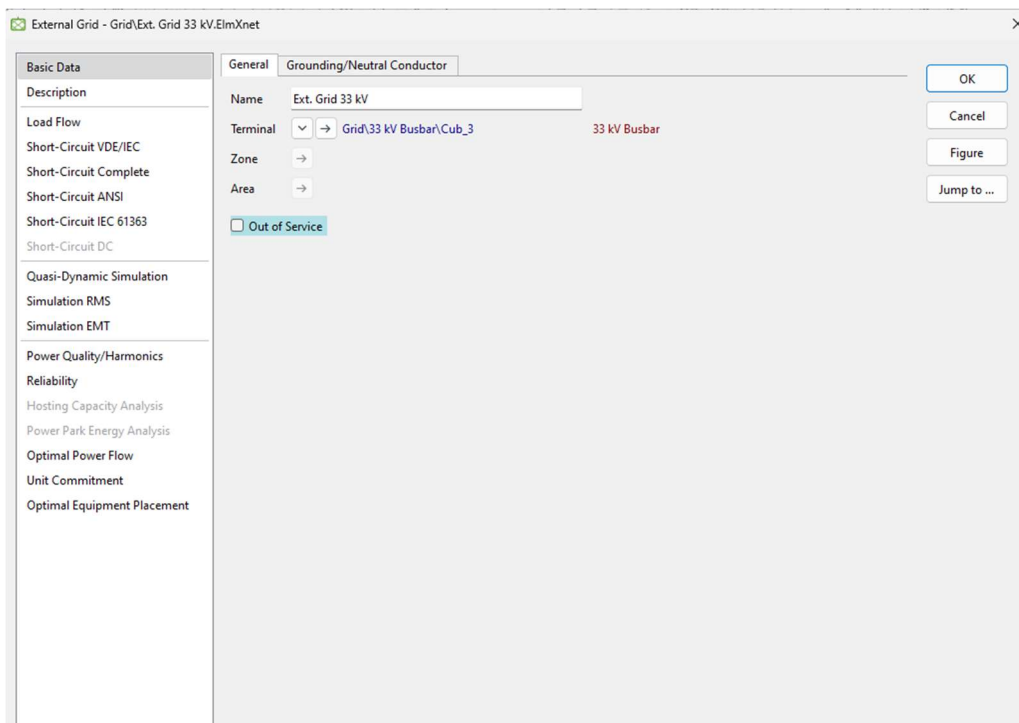


Fig. 4.1 Component Data Hierarchy in PowerFactory.

The window shown in the figure relates to the main network component. The data to be entered to define the element are divided according to their nature into different pages, listed in the left part of the window.

For example, data relative to power injection of a generator delivered in a certain moment of the operation are placed in the “Load-Flow” page, since this data is fundamental for load-flow simulations [21]. Each of the next paragraphs will be dedicated to entering the basic data of a single component of the network. The remaining data necessary to carry out the analysis will be introduced and discussed within the analysis chapter.

In the data exposure phases, it will be specified which of the data were not available from the project documentation made available by Loccioni, specifying the hypotheses or the other documentation consulted for the missing data.

## 4.2 Basic Data Setting of the components

### 4.2.1 Busbars

Within the network model, there are three main busbars to represent:

- 33 kV busbar
- 11 kV busbar
- 1kV Battery busbar

In this case, since the distances between these busbars are much shorter than the lengths of the radial network cables downstream the primary substation, there is no need to model any connecting line. Both the 33 kV and the battery busbars are therefore connected to the 11 kV busbar by means of transformers.

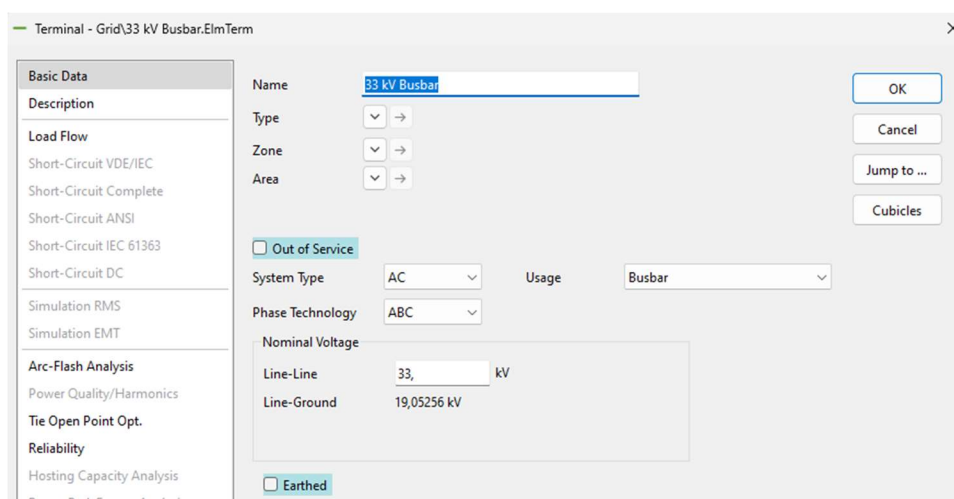


Figure 4.2 Terminal Basic Data.

In the Fig. 4.2 the basic data relative to the 33 kV busbar are shown. In this page it is important to specify the name of the busbar, the phase technology of the system, whether the system works in alternating or direct current, and the line-to-line nominal voltage of the element. There's also the opportunity to define the busbar as part of a certain zone or area of the network, and to put the component out of service. The basic data window of the other busbars are equal to the one shown.

## 4.2.2 External Grid

The main grid is represented by an external source element, connected to the 33 kV busbar.

The figure displays two screenshots of a software interface for configuring an external grid. The left screenshot shows the 'General' tab with the following fields: Name (Ext. Grid 33 kV), Terminal (Grid\33 kV Busbar\Cub\_3), Zone, Area, and an 'Out of Service' checkbox. The right screenshot shows the 'Grounding/Neutral Conductor' tab with the following settings: Neutral Conductor, N-Connection (None), Internal Grounding Impedance (Star Point: Connected), Petersen Coil (unchecked), Resistance, Re (0 Ohm), and Reactance, Xe (0 Ohm).

Figure 4.3, 4.4 External Grid Basic Data.

The External Grid basic data are divided in two different windows. In the “General” window the name of the element must be entered. The second window refers to grounding impedance and neutral conductor settings. The default data was left. In the current modeling step, the amount of data to be inserted is minimal; the component will be much more complex when the power generation strategies will be defined in the load-flow analysis.

## 4.2.3 Transformers

Transformers are more complex to model than the others seen previously and requires a premise: to describe integrally certain types of components, PowerFactory exploits two different objects, named “Type” and “Element” objects.

- Characteristic electrical parameters of a component are stored in the Type Object,
- Data relating to the topology or the operation scenarios (e.g., connections between component, length of a line, tap position of a transformer) are stored in the Element Object [21].

To completely define a transformer, there’s the need to define the Transformer Element and Type Objects. The transformer Type Object will be assigned to the transformer Element Object.

Parameter	Value	Unit
Name	HV tranformer Type	
Technology	Three Phase Transformer	
Rated Power	2,5	MVA
Nominal Frequency	50,	Hz
Rated Voltage (HV-Side)	33,	kV
Rated Voltage (LV-Side)	11,	kV
Vector Group (HV-Side)	Y	
Vector Group (LV-Side)	YN	
Phase Shift	0,	*30deg
Name	Yyn0	
Short-Circuit Voltage uk (Positive Sequence)	6,84	%
Copper Losses	20,	kW
Short-Circuit Voltage uk0 (Zero Sequence)	20,52	%
SHC-Voltage (Re(uk0)) uk0r	6,	%

Fig. 4.5 High Voltage Transformer Type Object Basic Data.

Fig. 4.5 is the page relative to the basic data options of the High Voltage Transformer Type Object. As clear from the image above, the data to be entered are purely electric, such as the rated power, the rated voltages the characteristic vector group and so on. It is possible to see here that the transformer is equipped with a neutral connection in the low voltage-side.

The basic data option of the element object of the transformer are divided in two pages: the General page and the Grounding/Neutral Conductor page. In the General page (Fig. 4.6) it is possible to define the connection of the transformer between the chosen busbars in the LV and HV sides. In the Grounding/Neutral Conductor page (Fig. 4.7) it is possible to define the node to which to connect the neutral conductor. In this case the neutral conductor is placed at the secondary winding of the transformer.

General Grounding/Neutral Conductor

Name: HV Transformer

Type: Equipment Type Library\HV transformer Type

HV-Side: Grid\33 kV Busbar\Cub\_2 33 kV Busbar

LV-Side: Grid\11 kV Busbar\Cub\_11 11 kV Busbar

Zone: HV-Side

Area: HV-Side

Out of Service

Number of parallel Transformers: 1

Flip Connections

Thermal Rating: [dropdown]

Meteo. Station: [dropdown]

Rating Factor: 1, Nominal Power (act.): 2,5 MVA

Supplied Elements

Mark Elements in Graphic Edit Elements

Fig. 4.6 High Voltage Transformer Element Object Basic Data, General Page.

General Grounding/Neutral Conductor

Neutral Conductor

N-Connection: Separate on LV

LV-Neutral: Grid\HV earthing node 1\Cub\_2 HV earthing node 1

Internal Grounding Impedance, LV Side

Star Point: Not connected

Fig. 4.7 High Voltage Transformer Element Object Basic Data, Grounding/Neutral Conductor.

All the images reported above in this paragraph are related to the 33/11 kV transformer. In the following, it is shown all the useful data that regard the 11/1 kV BESS transformer.

Name	BESS Transformer Type		OK
Technology	Three Phase Transformer		Cancel
Rated Power	3,	MVA	
Nominal Frequency	50,	Hz	
Rated Voltage		Vector Group	
HV-Side	11,	kV	HV-Side YN
LV-Side	1,	kV	LV-Side D
Positive Sequence Impedance		Phase Shift 0, *30deg	
Short-Circuit Voltage uk	6,	%	Name YNd0
Copper Losses	15,	kW	
Zero Sequence Impedance			
Short-Circuit Voltage uk0	8,	%	
SHC-Voltage (Re(uk0)) uk0r	2,	%	

Fig. 4.8 BESS Transformer Type Object Basic Data.

General		Grounding/Neutral Conductor		OK
Name	BESS Transformer			Cancel
Type	Equipment Type Library\BESS Transformer Type			Figure
HV-Side	Grid\11 kV Busbar\Cub_6	11 kV Busbar		Jump to ...
LV-Side	Grid\Battery Busbar\Cub_4	Battery Busbar		
Zone	HV-Side			
Area	HV-Side			
<input type="checkbox"/> Out of Service				
Number of parallel Transformers	1	Flip Connections		
Thermal Rating				
Meteo. Station				
Rating Factor	1,	Nominal Power (act.)	3, MVA	
Supplied Elements				
Mark Elements in Graphic		Edit Elements		

Fig. 4.9 BESS Transformer Element Object Basic Data, General Page.

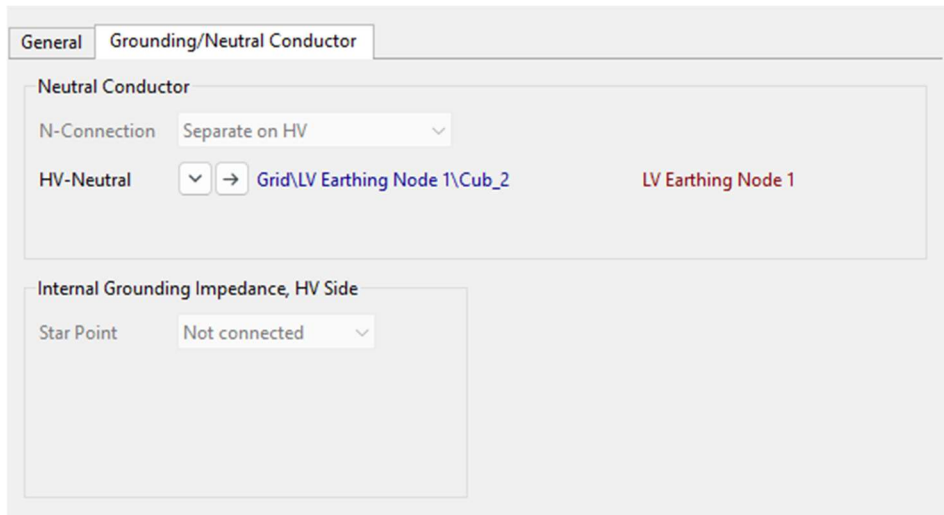


Fig. 4.10 BESS Transformer Element Object Basic Data, Grounding/Neutral Conductor.

#### 4.2.4 Earth connections

In the primary substation, both the 33 kV / 11 kV transformer and the 11 kV / 1 kV BESS transformer are equipped with grounding connections. While for the former this connection is installed in the secondary windings, in the BESS transformer the grounding conductor is installed on the primary windings.

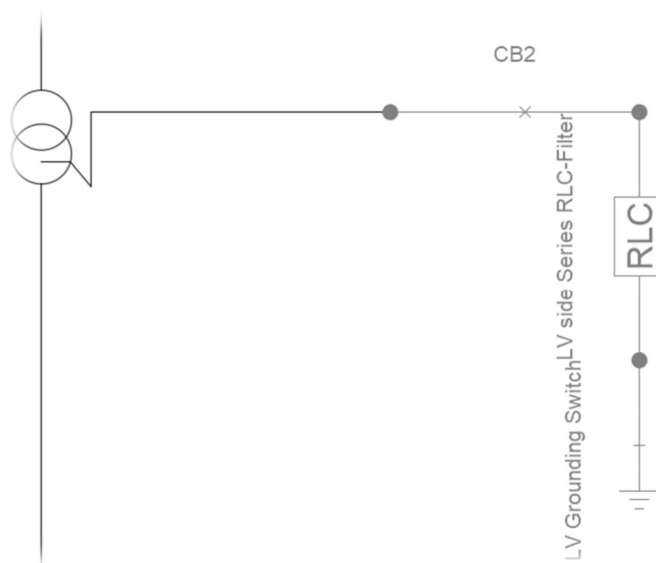


Fig 4.11 BESS Transformer Earthing connection.



The grounding was modeled through the union of three components using internal nodes:

- Switch
- RLC filter
- Grounding switch

In this preliminary phase of system modeling, the useful information to report for grounding is mainly the state of the switches, the nominal voltage and the number of phases of the ground connection. For the Load-Flow analysis, it is anticipated that the earth connections will have zero impedance.

The images relating to the basic data of each component are shown in the figures from Fig. 4.12 to Fig. 4.17.

The screenshot shows the configuration for a circuit breaker named 'CB1'. The 'Type' is set to 'Circuit-Breaker'. Terminal 'i' is connected to 'Grid\HV earthing node 2\Cub\_1' (HV earthing node 2), and Terminal 'j' is connected to 'Grid\HV earthing node 1\Cub\_1' (HV earthing node 1). The 'Actual State' is 'closed'. The 'No. of Phases' is 1 and 'No. of Neutrals' is 0. The 'Switch Type' is 'Circuit-Breaker'. Other options include 'Closed' (checked), 'Detailed for calculation' (unchecked), and 'Excluded from Running Arrangement' (unchecked).

Fig. 4.12 High Voltage Transformer Earthing Connection Circuit Breaker, Basic Data.

The screenshot shows the configuration for an 'HV side Series RLC-Filter'. Terminal 'i' is connected to 'Grid\HV earthing node 2\Cub\_2' (HV earthing node 2), and Terminal 'j' is connected to 'Grid\HV earthing node 3\Cub\_1' (HV earthing node 3). The 'Out of Service' checkbox is unchecked. The 'Ratings' section shows a 'Rated Voltage' of 11 kV (Line-Line Voltage) and a 'Rated Current' of 1 kA. The 'System Type' is 'AC' and 'Phases' is 1.

Fig. 4.13 High Voltage Transformer Series RLC Filter, Basic Data.

Name: HV Grounding Switch

Terminal: Grid\HV earthing node 3\Cub\_2 HV earthing node 3

Zone: →

Area: →

Closed

Detailed for calculation

No. of Phases: 1 No. of Neutrals: 0

Fig. 4.14 High Voltage Transformer Grounding Switch, Basic Data.

Name: CB2

Type: →

Terminal i: Grid\LV Earthing Node 1\Cub\_1 LV Earthing Node 1

Terminal j: Grid\LV Earthing Node 2\Cub\_1 LV Earthing Node 2

Zone: Terminal i →

Area: Terminal i →

Bay: →

Closed Actual State closed

Detailed for calculation

No. of Phases: 1 No. of Neutrals: 0

Switch Type: Circuit-Breaker

Excluded from Running Arrangement

Fig. 4.15 BESS Transformer Earthing Connection Circuit Breaker, Basic Data.

The screenshot shows the configuration form for a BESS Transformer Series RLC Filter. The name is "BESS side Series RLC-Filter". Terminal i is "Grid\LV Earthing Node 2\Cub\_2" (LV Earthing Node 2) and Terminal j is "Grid\LV Earthing Node 3\Cub\_1" (LV Earthing Node 3). Zone and Area are both set to "Terminal i". The "Out of Service" checkbox is unchecked. The Ratings section shows a Rated Voltage of 11 kV (Line-Line Voltage) and a Rated Current of 1 kA. Thermal Rating is set to "Terminal i", System Type is "AC", and Phases is "1".

Fig. 4.16 BESS Transformer Series RLC Filter, Basic Data.

The screenshot shows the configuration form for a BESS Transformer Grounding Switch. The name is "LV Grounding Switch". Terminal is "Grid\LV Earthing Node 3\Cub\_2" (LV Earthing Node 3). Zone and Area are both set to "Terminal i". The "Closed" checkbox is checked, and "Detailed for calculation" is unchecked. The No. of Phases is "1" and the No. of Neutrals is "0".

Fig. 4.17 BESS Transformer Grounding Switch, Basic Data.

## 4.2.5 BESS

The storage system is connected to the 1 kV busbar, together with the load relating to the auxiliaries.

Power Factory does not directly have a component relating to storage systems, but provides the component called "Static Generator" for the representation of these elements [22].

In this case, the main data to be entered in the Basic Data page are the plant category, the rated apparent power and the rated power factor, numbers of parallel units and the name of the terminal to which the BESS is connected.

General Zero Sequence/Neutral Conductor

Name: BESS

Terminal: Grid\Battery Busbar\Cub\_1 Battery Busbar

Zone: →

Area: →

Out of Service

Technology: 3PH

Plant Category: Storage Subcategory: →

Number of parallel units: 1

Ratings

Rated Apparent Power: 3, MVA

Rated Power Factor: 0,9

Model: →

Fig. 4.18 BESS Basic Data, General page.

#### 4.2.6 Neutral Earthing Compensator/Resistor

The neutral earthing compensator/resistor is used in electricity transmission and distribution systems to manage the currents during a ground fault. By modifying the reactance or resistance values of the neutral conductor, it modifies the earth fault current to a certain value, that must be neither too high as to damage the circuit, nor too low as not to trigger the protections when this type of fault occurs [23], [24].

General Grounding/Neutral Conductor

Name: NEC/NER

Terminal: Grid\11 kV Busbar\Cub\_10 11 kV Busbar

Zone: →

Area: →

Out of Service

Rated Voltage: 11, kV

Rated Current ( $I_e=3 \cdot I_0$ ): 0,1 kA

Zero Sequence Resistance: 0, Ohm

Zero Sequence Reactance: 0, Ohm

General Grounding/Neutral Conductor

Neutral Conductor

N-Connection: None

Internal Grounding Impedance

Star Point: Connected

Petersen Coil

Resistance,  $R_e$ : 0, Ohm

Reactance,  $X_e$ : 0, Ohm

1 Fig. 4.19, 4.20 NEC/NER Basic Data, General and Grounding/Neutral Conductor page.

Above, both pages relating to the basic data option are shown. In them data relating to the nominal current and voltage, the resistance and reactance values and the topological must be entered. Given that this

component does not influence the load-flow analysis and that earth faults will not be treated in the short-circuit analysis, this component does not influence the results of the analyses that will be explained later. For this reason, the default values have been maintained.

## 4.2.7 Auxiliary Load

For the correct functioning of the BESS, auxiliary components need to be installed. In fact, these types of systems are equipped with components such as the fire prevention system, video surveillance, battery cooling systems, lighting systems, HVAC (Heating, Ventilation and Air Conditioning) and UPS (Uninterruptible Power Supply) to power the emergency circuit and control components without interruptions. These components have been grouped in PowerFactory into a single general load object. the basic data are shown in Fig. 4.21.

The screenshot shows a software dialog box for configuring an Auxiliary Load. The fields are as follows:

- Name:** Auxiliary Load
- Type:** (dropdown menu)
- Terminal:** Grid\Battery Busbar\Cub\_2 (with a red label 'Battery Busbar' next to it)
- Zone:** (dropdown menu)
- Area:** (dropdown menu)
- Out of Service
- Technology:** 3PH-'D'
- Consider Load Transformer

On the right side of the dialog, there are four buttons: OK, Cancel, Figure, and Jump to ...

Fig. 4.21 Auxiliary Load Basic Data.

# Chapter 5: Distribution System Equivalent Model

The physical and electrical data of a distribution system are, most of the time, kept secret for security reasons. The exposure of such data requires the possession of permissions by the owner of the network. Since such permissions are not available, the real distribution system cannot be analysed directly in this study. Therefore, an equivalent system of the real network has been modeled. The modeling procedure is discussed in detail in the present paragraph.

The real model in possession does not show all the branches from the Bess station to the individual customer, but it just gives all the topological and electrical data related to the lines at the 11 kV voltage level. The loads present in the distribution network are grouped into more than 130 load blocks.

The first step to model the equivalent circuit is to decide the simplification level of it. In other words, choices regarding the number of nodes and lines joined and represented in the study should be taken. Two feeders depart from the BESS station, which branch into four main backbones, each having a high number of branches. Therefore, the model has been simplified by incorporating the properties of the small secondary branches into the network backbones. This has required the calculation of the equivalent impedance between lines in parallel or in series and the aggregate load calculation. The tabulation has been performed in Excel.

Knowing how PowerFactory models line elements is crucial to make the mathematics. Fig. 5.1 shows the lumped parameter model for a single-phase AC line.

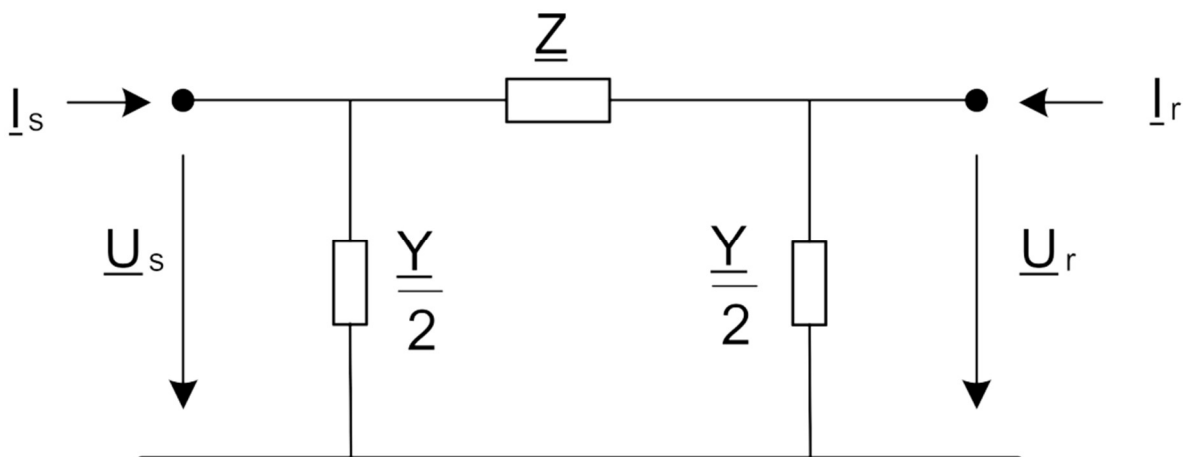


Figure 5.1 Lumped parameter model for a single-phase AC line. [25]

This parameter arrangement is valid also for three-phase systems. The line is characterized by its phase impedance, named “ $Z$ ” and by its admittance with respect to the ground “ $Y$ ”, divided in two blocks inside the model. In detail:

$$Z = Z' \cdot l = (R' + j\omega L') \cdot l \quad (5.1)$$

$$Y = Y' \cdot l = (G' + j\omega C') \cdot l \quad (5.2)$$

$$G' = B' \cdot \operatorname{tg} \delta \quad (5.3) [25]$$

The apostrophe on the quantities indicates that they are parameters per unit of length. “*l*” is the length of the line. The conductance is function of the susceptance and the insulation factor. In this study the insulation factor is assumed to be equal to zero. Although dealing with underground cables, given the low voltage level, the capacitive effects between phases and earth can be considered negligible. Once the equivalent network had been modelled, a brief confirmatory parametric analysis was carried out, implementing load-flow analysis for a wide range of capacities per unit of meter. This procedure confirms the initial hypothesis. The parameter to be evaluated are therefore *R'* and *L'*.

Through calculations, five different Line Types has been defined:

*Table 5.1 Resistances and Reactances per unit meter for the equivalent Line Type.*

Line Type	<i>R'</i> (Ω/km)	<i>X'</i> (Ω/km)
1	1,866	0,354
2	1,449	0,276
3	0,75	0,39
4	1,222	0,402
5	0,197	0,122

As for transformers, each line Type Object must be assigned to its proper line Element Object, according to the topology chosen. In PowerFactory, in the line Element Object are stored topological information and the line length, while the line Type Object contains all the electrical and physical parameters of the cables. For complete modeling of pipe, each line Type Object should be assigned to its relative line Element Object [21], as shown in Table 5.2.

*Table 5.2 Line Element and Type Association, Line Length.*

Line Element	Line Type	Line Element Length (km)
L1	5	1,12
L1_1	2	4,03
L1_2	1	7,98
L2	3	5,15
L2_1	3	4,3
L2_2	4	3,03

The last step to realize the equivalent network is to evaluate the equivalent aggregate load to each line. This is done by summing all the contributions by each local load presents in the network. A wind generator with nominal power of 0,73 MVA is connected to L2\_1. This is the only distributed energy resource present in the distribution network. This unit will be coordinated together with the external grid and the BESS to fulfill the total demand. In the study performed by the DNO on the meshed grid exploited to extract the network information useful for the current study purpose, all loads have the same power factor, equal to 0,98 [19]. The maximum demand of each aggregate load is shown in Table 5.3.

Table 5.3 Load names, Load Lines and Apparent Power of the Loads.

Name of Load/Generator	Line connected to the load	Maximum power (MVA)
1A	L1_1	0,77
1B	L1_2	0,265
2A	L2_1	0,566
2B	L2_2	0,184
WT	L2_1	0,73

Once aggregated the load relative to each line, five different transformers have been dimensioned according to the load demand and wind generator nominal power. 1 MVA transformers for the loads and 1,5 MVA transformer for the wind turbine has been chosen. The voltage of all the loads is equal to 0,4 kV. To enter the remaining transformer data, datasheets of real transformers available on the market with similar dimensions has been checked [26]. In the following, the relevant figures relative to the transformer type have been reported.

The image shows a software configuration window for a transformer. The fields are as follows:

- Name: T1\_5MVA
- Technology: Three Phase Transformer
- Rated Power: 1,5 MVA
- Nominal Frequency: 50 Hz
- Rated Voltage:
  - HV-Side: 11 kV
  - LV-Side: 0,4 kV
- Vector Group:
  - HV-Side: D
  - LV-Side: YN
- Phase Shift: 1, \*30deg
- Name: Dyn1
- Positive Sequence Impedance:
  - Short-Circuit Voltage uk: 4,75 %
  - Copper Losses: 5,6 kW
- Zero Sequence Impedance:
  - Short-Circuit Voltage uk0: 4,75 %
  - SHC-Voltage (Re(uk0)) uk0r: 2,025 %

Fig. 5.2 Load Transformer Type Object, Basic Data.



Name	TIMVA	
Technology	Three Phase Transformer	
Rated Power	1,	MVA
Nominal Frequency	50,	Hz
Rated Voltage		Vector Group
HV-Side	11,	kV
LV-Side	0,4	kV
Positive Sequence Impedance		HV-Side
Short-Circuit Voltage uk	6,	%
Copper Losses	4,5	kW
Zero Sequence Impedance		LV-Side
Short-Circuit Voltage uk0	4,75	%
SHC-Voltage (Re(uk0)) uk0r	2,025	%
		Phase Shift
		1,
		*30deg
		Name
		Dyn1

Fig. 5.3 Wind Generation Transformer Type Object, Basic Data.

All the parameters needed to graphically represent the equivalent model are now available. Fig. 5.4 illustrates the equivalent model designed in PowerFactory.

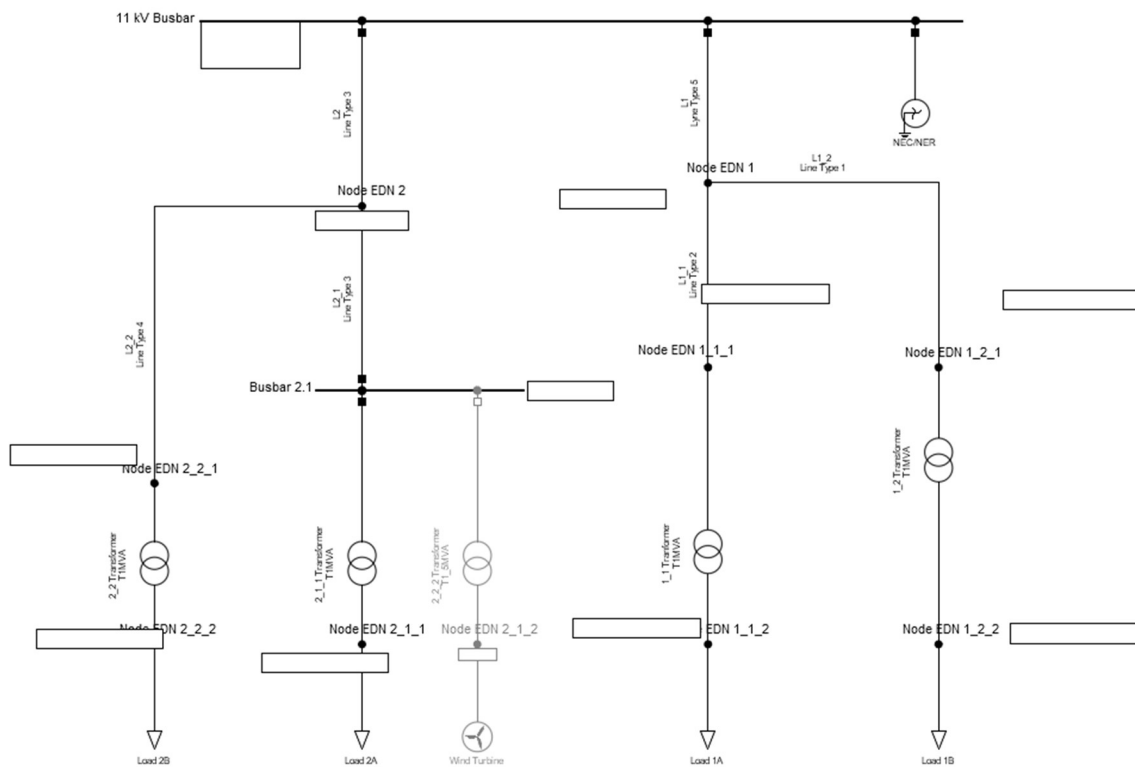


Fig. 5.4 Equivalent Distribution Network Model.

In conclusion, there is the need to evaluate the rated current of the equivalent conductors. This parameter is fundamental in load-flow analysis to understand the level of load exerted on the line. Since the conductors are made of copper and they are underground single-core cables, the resistance and reactance values of the equivalent lines can be compared to those of cables available on the market to obtain their section and, consequently, the nominal currents. Table 5.4 shows the current values relating to each line type and element.

*Table 5.4 Line Rated Current.*

<b>Line Element</b>	<b>Line Type</b>	<b>Rated Current (kA)</b>
L1	5	0,234
L1_1	2	0,071
L1_2	1	0,071
L2	3	0,127
L2_1	3	0,127
L2_2	4	0,096



# Part 3: Analysis Part

## Chapter 6: Load-Flow Analysis

### 6.1 Load-Flow Introduction

Load-flow analysis is a basic tool for the evaluation of power systems in steady-state conditions. The study evaluates how the equipment in the power system are loaded to meet demand. Through this method, it is possible to identify any weaknesses and develop countermeasure. Furthermore, it assesses the voltage levels of the grid, determining if they are within the acceptable limits.

Load-flow can be used for several applications, which can be classified based on whether they occur in normal state condition or during fault condition. If the grid works in normal operating conditions, load-flow can analyse the behavior of the system by calculating voltage drops, power losses and loadings on each component. Therefore, the load-flow method can be used in system optimization; by knowing the load-flow results, the operator can modify the parameters to find the optimum between system losses, generation costs and reliability of the system.

Beyond normal operation, it could be interesting to analyse the system behavior under fault conditions. The operators aim to understand how and if the system could meet demand in anomalous state caused by any kind of fault. Typically, an outage can cause the overload of the system, threatening the security of the network. Performing the load-flow analysis on a network with some branches disconnected gives precious information on supply uncertainty. With these results, operators can decide the best actions to be performed (e.g., system empowerment, protection settings etc.).

The results of the study can be useful both for systems already in operation and for those in the process of being designed.

Load-flow analysis is useful as the initial steady-state condition for other types of analysis, such as quasi-dynamic simulation, short-circuit and electromagnetic transient analysis [21].

Through the load-flow analysis, the most relevant operation scenarios of the network are evaluated and discussed. As expressed before, the microgrid can be connected to the national grid or can operate in islanded mode. Each of the cases are analysed individually. In the first case, the BESS provides only the energy necessary for load peaks or to improve the quality of voltage in the nodes of the electricity grid. In the second case, the BESS, in cooperation with the DER in the distribution network, provides the energy necessary to cover the load.

The operation scenarios are not characterized exclusively by whether the microgrid is connected to the national grid or not, but various load and distributed generation cases are also considered.

As regards loads, two cases will be presented: in the first, the average electrical load recorded in recent years are used, while in the second, the maximum load recorded is adopted.

Finally, within the network the wind generation (WG) can be disconnected from the network or not.

The drivers presented has been combined to define eight different operation scenarios, which have been evaluated through load-flow analysis:

- Case 1: Connected grid, Average load, Wind Generation
- Case 2: Disconnected grid, Average load, Wind Generation
- Case 3: Connected grid, Maximum load, Wind Generation
- Case 4: Disconnected grid, Maximum load, Wind Generation
- Case 5: Connected grid, Average load, No Wind Generation
- Case 6: Disconnected grid, Average load, No Wind Generation
- Case 7: Connected grid, Maximum load, No Wind Generation
- Case 8: Disconnected grid, Maximum load, No Wind Generation

The structure of the part is anticipated; first, the mathematical model behind the load-flow analysis is explained in detail. Following this, there is a step-by-step explanation on how to implement load-flow analysis within the software, focusing on the general settings, the settings of the load-flow command and the settings of each component present within the network. Finally, the results of each case study are compared and discussed.

## 6.2 Load-Flow Mathematical Model

Load-flow analysis is used to calculate the voltage values  $V$ , phase angles  $\delta$ , active and reactive power  $P$  and  $Q$  in each component of the power system.

Before the analysis, the operator only partially knows the value of these quantities. Buses within the network are classified according to which of their parameters must be determined:

- Slack (SL) Buses: Slack bus is usually connected to a generator and is the bus chosen as a reference. Its phase angle  $\delta$  is known as well as its voltage magnitude. The generation is adjusted to ensure power balance.
- Generator (PV) Buses: PV Buses, like the Slack Buses, are connected to generator units, and its generation could be modulated to match the power demand. It is known the active power and the voltage magnitude of this type of bus, but the reactive power and the phase angle are unknown.
- Load (PQ) Buses: PQ buses are those connected to a load. The load value is an input of the load-flow analysis. It can be a forecast or an actual value. The unknown variables are  $V$  and  $\delta$ .

A summary table on the bus classification is reported in Table 6.1.

Table 6.1 Bus Classification. [27]

Table 1. Bus classification.					
No.	Type of Bus	Variables			
		$P$	$Q$	$ V $	$\delta$
1	Slack Bus	Unknown	Unknown	Known	Known
2	Generator Bus (PV)	Known	Unknown	Known	Unknown
3	Load Bus (PQ)	Known	Known	Unknown	Unknown

Performing a load-flow analysis means to define and to solve a set of nodal equations. This system can be represented in the matrix form:

$$I = [Y]V \quad (6.1)$$

where " $I$ " is the current array, " $V$ " is the voltage array and " $[Y]$ " is the admittance matrix of the system. Inside the expression lie the topological and electrical relationships between nodes.

For an  $N$  bus system, the nodal equation can be written as:

$$I_i = \sum_{j=1}^N Y_{ij} V_j \quad \text{for } i = 1, 2 \dots N \quad (6.2)$$

and since:

$$P_i + jQ_i = V_i I_i^* \quad (6.3)$$

$$I_i = \frac{P_i - jQ_i}{V_i^*} \quad (6.4)$$

it is possible to apply the substitution:

$$\frac{P_i - jQ_i}{V_i^*} = V_i \sum_{j=1}^N Y_{ij} - \sum_{j=1}^N Y_{ij} V_j \quad (6.5)$$

The above equation can be solved by iterative method. the most used iterative methods are the Gauss-Seidel Method, the Fast Decoupled Method and the Newton-Raphson Method. In the case study, the last-mentioned method has been implemented [27].

The Newton-Raphson Method approximate a non-linear equation system to a set of linear equations using a first order Taylor's series expansions. It is widely used in load-flow calculations since is one of the best methods in terms of convergence characteristics. Its computational speed depends on the distance between the guessed solution and the real one [6].

Considering a set of n non-linear algebraic equations, at node  $i$ :

$$f_i(x_1, x_2, \dots, x_N); \quad i = 1, 2, \dots, N \quad (6.6)$$

and assuming initial values of unknowns  $x_1^0, x_2^0, \dots, x_N^0$

assuming also a set of corrections for the assumed values  $\Delta x_1^0, \Delta x_2^0, \dots, \Delta x_N^0$

it is possible to approximate the equations to a first order Taylor series:

$$f_i(x_1^0 + \Delta x_1^0, x_2^0 + \Delta x_2^0, \dots, x_N^0 + \Delta x_N^0) + \left[ \left( \frac{\partial f_i}{\partial x_1} \right)^0 \Delta x_1^0 + \left( \frac{\partial f_i}{\partial x_2} \right)^0 \Delta x_2^0 + \dots + \left( \frac{\partial f_i}{\partial x_N} \right)^0 \Delta x_N^0 \right] \approx 0 \quad (6.7)$$

Representing them in matrix form:

$$\begin{bmatrix} f_1^0 \\ f_2^0 \\ \dots \\ f_N^0 \end{bmatrix} + \begin{bmatrix} \left(\frac{\partial f_1}{\partial x_1}\right)^0 & \left(\frac{\partial f_1}{\partial x_2}\right)^0 & \dots & \left(\frac{\partial f_1}{\partial x_N}\right)^0 \\ \left(\frac{\partial f_2}{\partial x_1}\right)^0 & \left(\frac{\partial f_2}{\partial x_2}\right)^0 & \dots & \left(\frac{\partial f_2}{\partial x_N}\right)^0 \\ \dots & \dots & \dots & \dots \\ \left(\frac{\partial f_N}{\partial x_1}\right)^0 & \left(\frac{\partial f_N}{\partial x_2}\right)^0 & \dots & \left(\frac{\partial f_N}{\partial x_N}\right)^0 \end{bmatrix} \begin{bmatrix} \Delta x_1^0 \\ \Delta x_2^0 \\ \dots \\ \Delta x_N^0 \end{bmatrix} \approx \begin{bmatrix} 0 \\ 0 \\ \dots \\ 0 \end{bmatrix} \quad (6.8)$$

That is:

$$f^0 + J^0 \Delta x^0 \approx 0 \quad (6.9)$$

where  $J^0$  is the jacobian matrix. The equation can be also written as:

$$f^0 \approx [-J^0] \Delta x^0 \quad (6.10)$$

The values of  $x$  for the next iterative step are modified using the corrector value; at iteration  $t$ :

$$x^{t+1} = x^t + \Delta x^t \quad (6.11)$$

The method continues to iterate until the following inequality is verified [28]:

$$|f_i(x^t)| < \varepsilon \quad (6.12)$$

where  $\varepsilon$  is the desired accuracy and  $i$  is the index of the node.

Applying the method to the electricity network, the arrays  $x^t$  and  $x^{t+1}$  correspond to the vectors of the voltages  $V$  and angles  $\delta$  of the nodes at time steps  $t$  and  $t+1$  respectively. the function  $f^t$  is the vector of the active and reactive powers  $P$  and  $Q$  of the nodes at time step  $t$ . The components of such vector have the following formulas [27]:

$$P_i = \sum_{j=1}^N |V_i| |V_j| |Y_{ij}| \cos(\theta_{ij} - \delta_i + \delta_j) \quad (6.13)$$



$$Q_i = \sum_{j=1}^N |V_i| |V_j| |Y_{ij}| \sin(\theta_{ij} - \delta_i + \delta_j) \quad (6.14)$$

The Jacobian  $J^t$  is the matrix of the partial derivatives of the active and reactive powers  $P$  and  $Q$  with respect to the voltage  $V$  and angles  $\delta$  of the nodes at time step  $t$ .

## 6.3 Component settings for Load-Flow Analysis

In the first phase of network modeling, only the topological and electrical information of each component basic data page have been defined. This paragraph includes the remaining data necessary to perform the load-flow analysis. Like the basic data page, each component has its dedicated load-flow page.

For some components different settings are presented depending on the case study to be analysed. Furthermore, for the desired coordination of generation and to maintain an adequate voltage level on all nodes of the network, two new objects are defined: the virtual power plant (VVP) and the station controller.

### 6.3.1 Terminals

Fig. 6.1 Terminal Load-Flow Data.

Fig. 6.1 shows the Load-Flow page of the 33 kV busbar. In the top part all those fundamental parameters for the definition of voltage control are declared. In fact, a generator can modify its production to obtain a target voltage at a pre-established terminal. This action is crucial to keep all the node voltages within the acceptable limits. The values of “*delta V min*” and “*delta V max*” identify the maximum deviation allowable without incurring in software’s errors or warnings. In case the voltage control strategy involves more than one node or busbar, the priority number expresses the importance of the voltage targets within terminals: the lower the priority number, the higher the terminal priority.

In conclusion, for each terminal it is possible to define the upper and lower steady-state voltage limit.

## 6.3.2 External Grid

General Advanced Automatic Dispatch

External Station Controller

External Secondary Controller

Local controller settings have precedence since the external station controller is out of service.

Bus Type  Setpoint

Out of service when active power is zero

Operation Point

Input Mode

Active Power  MW

Reactive Power  Mvar

Voltage Setpoint  p.u.

Angle  deg

Reference Busbar

Primary Frequency Bias  MW/Hz

Secondary Frequency Bias  MW/Hz

Reactive Power Operational Limits

Capability Curve

Min.  Mvar Scaling Factor (min.)  %

Max.  Mvar Scaling Factor (max.)  %

Fig. 6.2 External Grid Load-Flow Data, General Page.

For an External Grid, the load-flow page is divided in turn into three different sections, which are the General, the Advanced and the Automatic Dispatch sections.

As it is possible to see from Fig. 6.2, the bus connected to the external grid has been defined as the Slack busbar. Apart from that, in the general section the operation point of the source is set, entering active and reactive power values, as well as the desired voltage at the busbar. A reference busbar could be chosen. In this case, the generator aims to inject the power required to make the terminal reach the voltage setpoint. The best voltage setpoint for the reference busbar depends on the power losses and therefore on the power fluxes flowing in the network. To avoid low voltage values at loads, the voltage setpoint at the 33 kV busbar has been set equal to 1,02 per unit.

Primary and secondary frequency bias are not treated in this study, since it is not the aim of this thesis to analyse the frequency behavior of the grid.

Finally, the Reactive Power Operational Limits can be set. Since this component represents the national grid, it has been decided to maintain the default values, where the high values in modulus of the limits indicate the ability to inject or absorb reactive power orders of magnitude greater than the microgrid power flows.

As regards the advanced page, for the moment it is enough to know that an  $R/X$  ratio of 0,2 is assumed. The choice is motivated by the high resistivity of the downstream network. The remaining data on this page are

explained in detail in the short-circuit analysis chapter. The Automatic Dispatch page, on the other hand, is connected to the Virtual Power Plant (VPP) component, which is described later.

The screenshot shows the 'Automatic Dispatch' tab with a dropdown menu set to 'Max. Values'. It is divided into two columns: 'Max. Values' and 'Min. Values'. Each column contains input fields for several parameters:

Parameter	Max. Value	Min. Value
Short-Circuit Power $S_k$	1428,942 MVA	1428,885 MVA
Short-Circuit Current $I_k$	25 kA	24,999 kA
c-Factor	1,01	1
R/X Ratio	0,2	0,2
Impedance Ratio		
Z2/Z1	1	1
X0/X1	1	1
R0/X0	0,1	0,1

Below these fields, there is a checkbox for 'Consider for region spinning reserve' (unchecked) and a 'Generation shift key' set to 100%.

Fig. 6.3 External Grid Load-Flow Data, Advanced Page.

The screenshot shows the 'Automatic Dispatch' tab with the following settings:

- Virtual Power Plant:** A dropdown menu is set to 'Virtual Power Plant'.
- Generator Dispatch:** Radio buttons for 'Fixed' and 'Dispatchable' are present, with 'Dispatchable' selected.
- Merit Order:** A text input field contains the value '1'.
- Must run:** A checkbox is checked.
- Active Power Operational Limits:** A section with a gear icon containing:
  - Min. 0 MW
  - Max. 100000 MW

Fig. 6.4 External Grid Load-Flow Data, Automatic Dispatch.

### 6.3.4 Transformers

To set correctly the transformers for the load-flow analysis in the Software, it is important to remember that these components are defined assigning a Type Object to an Element Object [21]. The Type Object load-flow page is divided into four sections named General, Tap Changer, Saturation and Advanced sections.

What is important to highlight here is the tap changer at the HV side of the transformer. Modifying the tap position changes the transformation ratio of the component. This will be a variable for the software to keep the required voltage levels within the network. In the General section, parameters related to the magnetizing impedance and the distribution of leakage reactances can be set. For the latter, the default values have been kept.

The load-flow page of the Element Object is divided into four different sections. In them it is possible to set the maximum and minimum position of the tap changer, the initial tap position and so on. In the “Controller, Tap Changer 1” section it is possible to set the control on the tap. In fact, the tap position could be controlled by and external tap controller, by an external station controller, by an external LCC controller or by means of automatic tap changing control. For the latter options, parameters such as the winding to be controlled, the voltage setpoint and the lower and upper voltage bounds must be set. Whenever the reference voltage value goes outside the limits, the automatic control changes the position of the tap to try to bring the reference phase back within the limits. For the moment, no tap changer control strategy is chosen.

For a compact presentation, only the data relating to the 33 kV / 11 kV transformer is shown in its entirety. For the BESS transformer, the wind turbine transformer and the transformers connected to a load, only the general page of the Type Object is shown, since the remaining pages are similar to the ones related to the 33 kV / 11 kV transformer.

The figure displays two screenshots of a software interface for configuring a High Voltage Transformer Type Object. The left screenshot shows the 'General' tab with the following parameters:

Magnetising Impedance		Zero Sequence Magnetising Impedance	
No Load Current	3, %	Mag. Impedance/uk0	0,
No Load Losses	1,5 kW	Mag. R/X	0,

Below these are sections for 'Distribution of Leakage Reactances (p.u.)' and 'Distribution of Leakage Resistances (p.u.)', both with HV-Side and LV-Side values set to 0,5.

The right screenshot shows the 'Tap Changer' tab with the following parameters:

Tap Changer 1	
Type	Ratio/Asym. Phase Shifter
at Side	HV
Additional Voltage per Tap	2,5 %
Phase of du	0, deg
Neutral Position	0
Minimum Position	-2
Maximum Position	2

Fig. 6.5, 6.6 High Voltage Transformer Type Object Load Flow Data, General and Tap Changer Page.

General | Controller, Tap Changer 1 | Controller, Tap Changer 2 | Advanced

Tap Changer 1

Neutral: 0 Min: -2 Max: 2  
 Additional Voltage per Tap 2,5 %  
 Phase of du 0, deg

Tap Position 0

According to Measurement Report

Operational limits for tap changer

Tap Changer 1

Minimum Position -2  
 Maximum Position 2

Thermal Loading Limit

Max. loading 100, %

Loss assignment according to grouping

External Tap Controller [v] [→]  
 External Station Controller [→]  
 External LCC Controller [→]

Automatic Tap Changing

Fig. 6.7, 6.8 High Voltage Transformer Element Object Load-Flow Data, General and Controller, Tap Changer 1 Page.

General | Tap Changer | Saturation | Advanced

Magnetising Impedance

No Load Current 3, %  
 No Load Losses 2,5 kW

Distribution of Leakage Reactances (p.u.)

x, Pos. Seq. HV-Side 0,5  
 x, Pos. Seq. LV-Side 0,5

Distribution of Leakage Resistances (p.u.)

r, Pos. Seq. HV-Side 0,5  
 r, Pos. Seq. LV-Side 0,5

General | Tap Changer | Saturation | Advanced

Magnetising Impedance

No Load Current 3, %  
 No Load Losses 1,5 kW

Distribution of Leakage Reactances (p.u.)

x, Pos. Seq. HV-Side 0,5  
 x, Pos. Seq. LV-Side 0,5

Distribution of Leakage Resistances (p.u.)

r, Pos. Seq. HV-Side 0,5  
 r, Pos. Seq. LV-Side 0,5

Fig. 6.9, 6.10 BESS Transformer and Load Transformer Type Object Load-Flow Data, General Page.

Magnetising Impedance	
No Load Current	3, <input type="text"/> %
No Load Losses	0,7 <input type="text"/> kW

Distribution of Leakage Reactances (p.u.)	
x,Pos.Seq. HV-Side	0,5 <input type="text"/>
x,Pos.Seq. LV-Side	0,5 <input type="text"/>

Distribution of Leakage Resistances (p.u.)	
r,Pos.Seq. HV-Side	0,5 <input type="text"/>
r,Pos.Seq. LV-Side	0,5 <input type="text"/>

Fig. 6.11 Wind Generation Transformer Type Object Load-Flow Data, General Page.

### 6.3.5 Loads

As mentioned in the introduction of the load-flow analysis chapter, two load cases are presented: the average load and the maximum load. The image relating to the load profile recorded from 2015 to 2019 is shown again in Fig. 6.11.

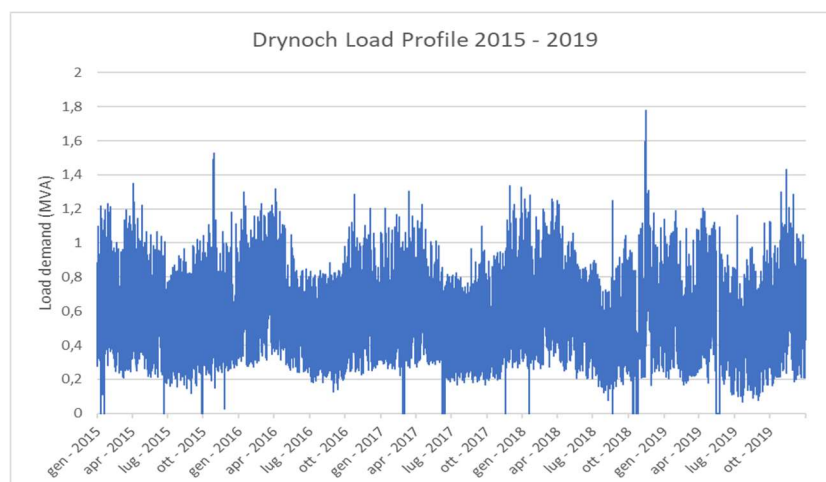


Fig. 6.12 Drynoch Load Data. [19].

It can be seen from the figure that the maximum peak of 1,78 MVA was reached in January 2019. The average load recorded is approximately 1 MVA.

Figure 6.12 shows the general load-flow page of the load downstream of branch L2\_2:

Fig. 6.13 Load-Flow Data of load 2B, General Page.

Here it is possible to define the operating point of the load, setting the apparent power, the power factor, the target voltage and the scaling factor.

In the documentation made available by Loccioni, the values of every single load on the network in the most critical scenario recorded are known. these loads were then aggregated and associated with the equivalent branch defined in the simplification phase of the real model. A power factor of 0.98 for all loads and a consumption of the BESS auxiliary systems of 100 kW are assumed. The maximum apparent power values of each load are shown in the table:

Table 6.1 Maximum Power of Loads.

Name of Load/Generator	Maximum power (MVA)
1A	0,77
1B	0,265
2A	0,566
2B	0,184
WT	0,73

In the general section of the load-flow page, it is possible to set the scaling factor value. the load value used in the analysis will be equal to the product between the apparent power entered and the scaling factor [21]. the ratio between the average load assumed and the maximum load is equal to  $1\text{MVA} / 1,78\text{MVA} = 0,56$ .

Once entered the maximum apparent power demanded by each aggregated load, by changing the scaling factor, it is possible to quickly switch from the maximum load case to the medium load case. In the first case, the scaling factor will be equal to 1, in the second case, it will be equal to 0.56.

The average load values of the aggregated load are listed below.

Table 6.2 Average Power of Loads.

Name of Load/Generator	Average Power (MVA)
1A	0,43
1B	0,15
2A	0,32
2B	0,103
WT	0,41

### 6.3.6 Wind Turbine

Fig. 6.14 Wind Generation Load-Flow Data, General Page.

In the distribution network there is a small wind turbine with an apparent nominal power of 0,73 MVA. A power factor equal to 1 is assumed. Here too, the power injected into the network can be modulated thanks to the scaling factor.

As with any type of static generator, local control of the generation can be defined. The turbine is operated at constant reactive power equal to zero.



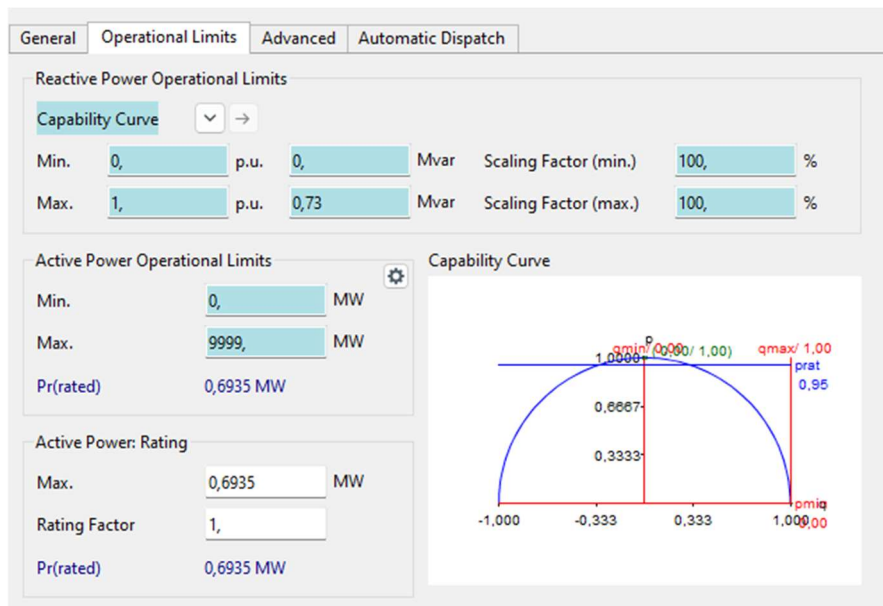


Fig. 6.15 Wind Generation Load-Flow Data, Operational Page.

In the Operational Limits page, the operation area of the turbine can be defined. The capability curve was not defined manually, it was enough to define the operation limits, so that the turbine can only inject power into the grid, without absorbing it.

### 6.3.7 Virtual Power Plant (VVP)

Virtual Power Plant are used in PowerFactory to group a set of generators to reach the desired active power. Through this component, it is possible to set some rules of dispatch. By assigning a merit order to each generator, it is possible to define which generator should run first with respect to the others. Since the wind generator will produce a priori the active power entered in the load-flow page if connected to the grid, there is no need to group it in the VVP. It is important to group both the external source and the BESS in the VVP, giving a higher merit order to the external source. By doing so, in case of parallel mode operation, the BESS will generate only the amount of active and reactive power declared in its load-flow page. In case of islanded mode, the external source will be out of service and the BESS will be taken as the reference machine of the grid. It means that the BESS will act as the slack generator and it will try to match the difference between the wind turbine generation and the load demand.

This setting can be kept fixed for all the operation scenarios.

### 6.3.8 Station Controller

The station controller object coordinates all the generator grouped in it. The aim is to keep a certain reference terminal at a target voltage defined by the user. The station controller therefore is used to control the reactive power injected by each generator. In this case only the external source and the BESS are controlled by it (as it is possible to see in the “Connected” column in Fig. 6.15). The user did not define the target node. Instead, during the load-flow analysis there is an automatic selection performed by the algorithm. This is named as Automatic Selection of the node.

The screenshot shows the 'Station Control' configuration window. The name is 'Station Control'. The 'Out of Service' checkbox is checked. Below is a table with columns 'Machines' and 'Connected'.

	Machines ElmSym,ElmGenstat,ElmPvsys,ElmSvs,ElmAsm,ElmVsc*,ElmX...	Connected
1	Wind Turbine	<input type="checkbox"/>
2	Ext. Grid 33 kV	<input checked="" type="checkbox"/>
3	BESS	<input checked="" type="checkbox"/>

Fig 6.16 Station Controller Basic Data.

The screenshot shows the 'General' tab of the 'Station Controller Load-Flow Data' configuration window. The 'Control Mode' is set to 'Voltage Control' and the 'Phase' is set to 'Pos.Seq.'. Under 'Controlled Node', 'Automatic Selection' is selected. The 'Busbar Search Criteria >=' is set to '0,1 kV'. A note says 'Press "Info" button to display controlled nodes.'

Fig 6.17 Station Controller Load-Flow Data, General Page.

## 6.3.9 BESS

Reference Machine  
 Out of service when active power is zero  
 Local Controller: Const. V  
 External Secondary Controller: [v] [→]  
 External Station Controller: [v] [→] Grid\Station Control  
 Quasi-Dynamic Model: [→] Grid\Battery Model  
 Local controller settings have precedence since the external station controller is out of service.

Dispatch		Actual Dispatch	
Input Mode	P, Q	Active Power (act.)	0, MW
Active Power	0, MW	Reactive Power (act.)	0,8 Mvar
Reactive Power	0,8 Mvar	Apparent Power (act.)	0,8 MVA
Voltage	1,02 p.u.	Power Factor (act.)	0, ind.
Angle	0, deg	Scaling Factor (act.)	1,
Prim. Frequency Bias	0, MW/Hz		
Scaling Factor	1,		

Fig. 6.18 BESS Load-Flow Data, General Page.

Being the BESS system modeled as a static generator as the wind turbine in PowerFactory, the Load-Flow pages of these components are like each other. The BESS is set as reference machine of the network only in islanded mode, while in case of parallel mode operation the external source is the slack generator. BESS always works at constant voltage, no matter the operation scenario. In the load-flow analysis, the active power injected by the energy storage system depends on the load demand, while the reactive power depends mainly on the voltage levels of the grid. In case of parallel mode operation and average load equal to 1 MVA, only the possible wind generator and the external source satisfy the active power demand. The BESS injects only reactive power to improve the voltage quality of the microgrid. The BESS injects active power in parallel mode operation only for maximum load operation scenario. It means that in these cases the BESS produces enough active power to cover the demand peaks. It has been decided that in these cases the BESS injects 0,4 MW.

In islanded mode, the BESS cooperates with the wind generator (if not out of service, depending on the operation scenario) to cover the demand, injecting the stored active power. For each case under study, the BESS provides reactive power to keep the voltage quality of the microgrid within acceptable limits.

Since the radial network of the microgrid is highly resistive, voltage drops can be considerable. In order not to have very low voltage values at the loads, a voltage value is therefore set in the battery terminal slightly higher than the nominal one, equal to 1,02 per unit.

The operational limits of the battery are in Fig. 6.19.

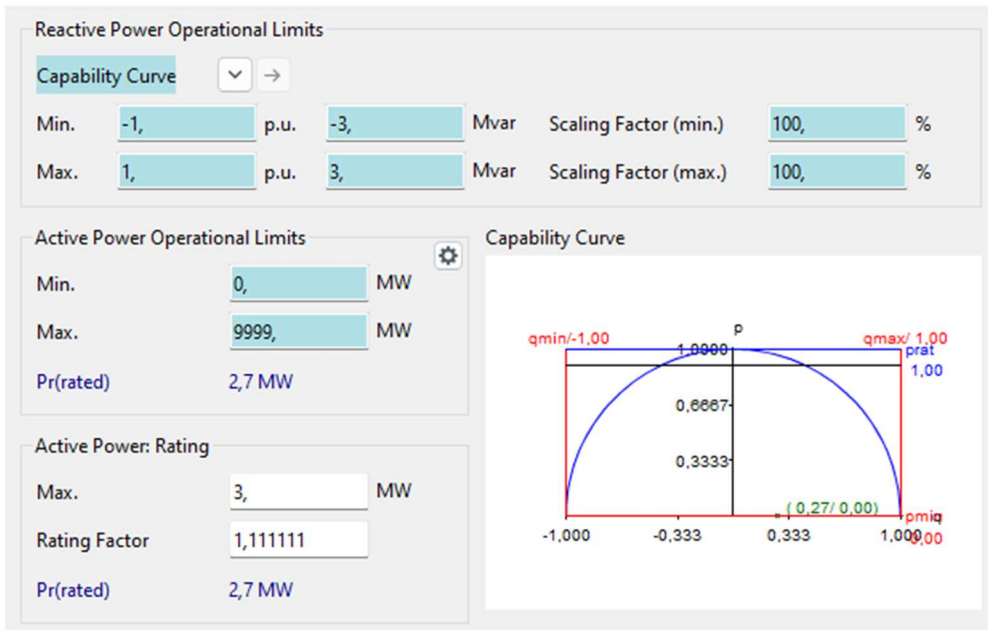
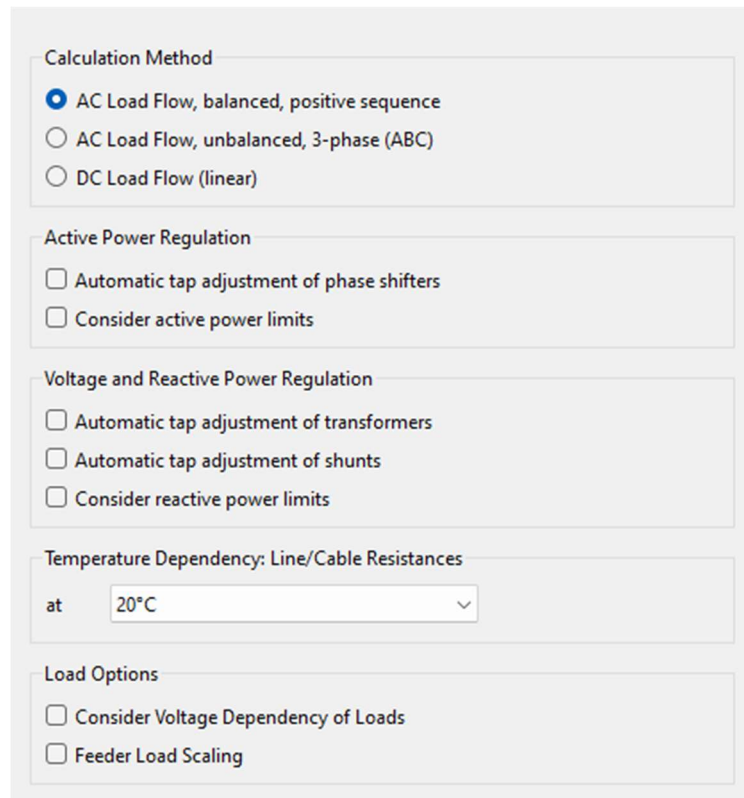


Fig. 6.19 BESS Load-Flow Data, Operational Limits Page.

## 6.4 Load-Flow Command Settings

Once all the data necessary to perform the load-flow calculation has been defined, it is time to set the load-flow calculation options. This is possible by opening the load-flow calculation icon. All the different settings are clustered into six different sections.



The screenshot shows a settings dialog box for load-flow calculation, organized into six sections:

- Calculation Method:** Three radio button options:  AC Load Flow, balanced, positive sequence;  AC Load Flow, unbalanced, 3-phase (ABC);  DC Load Flow (linear).
- Active Power Regulation:** Two checkbox options:  Automatic tap adjustment of phase shifters;  Consider active power limits.
- Voltage and Reactive Power Regulation:** Three checkbox options:  Automatic tap adjustment of transformers;  Automatic tap adjustment of shunts;  Consider reactive power limits.
- Temperature Dependency: Line/Cable Resistances:** A label 'at' followed by a dropdown menu showing '20°C'.
- Load Options:** Two checkbox options:  Consider Voltage Dependency of Loads;  Feeder Load Scaling.

Fig. 6.20 Load-Flow Command, Basic Data Page.

In the Basic Options, it is possible to define the Calculation Method by checking the boxes. In this case, it is needed to perform a balanced AC load-flow, imbalances between the three different phases are not going to be considered. Talking about the Active Power Regulation, it is possible to enable the automatic tap adjustment of phase shifters, as well as to consider active power limits define in the models of the generators. None of these options have been selected. Regarding the voltage and reactive power regulation, there is the option to enable the automatic tap adjustment of transformer. The tap adjustment is carried out according to the control settings defined in the transformer element's dialog. Reactive power limits are considered. If the load-flow cannot be solved without exceeding the reactive power limits defined in the models of the generators, the software returns an error message.

Since the electrical characteristics of lines and transformers are related to temperature, it is possible to change the temperature at which the analysis is carried out. In this case, a temperature of 20° C has been chosen.

In conclusion, in the Basic Options it could be chosen to consider voltage dependency of load and the feeder load scaling.

In the Active Power Control Page, it is possible to decide which kind of strategy to adopt to fulfill the load demand. Power generation can be divided between generators according to their inertias, or according to

primary or secondary control. In this case it has been chosen the “as dispatched active power control”: it means that the power balance is guaranteed by the slack generator. In case the grid under study is connected to the main grid, the external source is the slack generator. In islanded mode, the BESS plays this role. If as in this case the “as dispatched” control is selected, it is possible to define more options regarding the power balancing method. There is the option to choose between strategies on how to balance the losses within the network. In this case, all the losses are balanced by the reference machine.

Active Power Control

- as Dispatched
- according to Secondary Control
- according to Primary Control
- according to Inertias

Balancing

- by reference machine
- by load at reference bus
- by static generator at reference bus
- Distributed slack by loads
- Distributed slack by synchronous generators
- Distributed slack by synchronous generators and static generators

Reference Bus

Reference Busbar  →

Angle 0,  deg

Fig. 6.21 Load-Flow Command, Active Power Control Page.

Since the Advanced Options, Outputs and Load/Generation Scaling pages are not particularly important for the study under analysis, they will not be described. On the last relevant page, called Calculation Settings, two types of Newton-Raphson Method can be chosen: the classic one and a second called Current Equations Newton-Raphson Method. As expressed in the software manual, while the former reaches convergence faster in more complex networks, the latter is particularly accurate if simpler networks are being analysed [21]. Therefore, the Current Equation Method has been chosen.

Load Flow Method

- Newton-Raphson (Current Equations)
- Newton-Raphson (Power Equations, classical)

Fig. 6.22 Load-Flow Command, Calculation Settings Page.



In this chapter, the results of the analysis are presented and commented on. Node voltages, power line loadings and the network losses obtained are compared for each operational scenario.

Below there are the operational scenarios already introduced previously. For conciseness, the operation scenarios are referenced using codes:

- Case 1: Connected grid, Average load, Wind generation (1-Co-AL-WG)
- Case 2: Disconnected grid, Average load, Wind generation (2-Di-AL-WG)
- Case 3: Connected grid, Maximum load, Wind generation (3-Co-ML-WG)
- Case 4: disconnected grid, maximum load, wind generation (4-Di-ML-WG)
- Case 5: connected grid, average load, no wind generation (5-Co-AL-No WG)
- Case 6: disconnected grid, average load, no wind generation (6-Di-AL-No WG)
- Case 7: connected grid, maximum load, no wind generation (7-Co-ML-No WG)
- Case 8: disconnected grid, maximum load, no wind generation (8-Di-ML-No WG)

To begin with, a first table relating to the values of generated, absorbed and dispersed power of the system is reported in Table 6.3:

*Table 6.3 Network Power Flows.*

	Case 1	Case 2	Case 3	Case 4	Case 5	Case 6	Case 7	Case 8
	(1-Co-AL-WG)	(2-Di-AL-WG)	(3-Co-ML-WG)	(4-Di-ML-WG)	(5-Co-AL-No WG)	(6-Di-AL-No WG)	(7-Co-ML-No WG)	(8-Di-ML-No WG)
<b>P Ext Source (MW)</b>	0,383	0	0,821	0	1,116	0	1,54	0
<b>Q Ext Source (Mvar)</b>	0,162	0	0,227	0	0,105	0	0,188	0
<b>P BESS (MW)</b>	0	0,378	0,36	1,175	0	1,107	0,4	1,929
<b>Q BESS (Mvar)</b>	0,262	0,391	0,404	0,607	0,281	0,342	0,436	0,597
<b>P Wind Generation (MW)</b>	0,73	0,73	0,73	0,73	0	0	0	0
<b>Q Wind Generation (Mvar)</b>	0	0	0	0	0	0	0	0
<b>Total Load (MW)</b>	1,08	1,08	1,85	1,85	1,08	1,08	1,85	1,85
<b>Total Load (Mvar)</b>	0,2	0,2	0,36	0,36	0,2	0,2	0,36	0,36
<b>Total P Losses (MW)</b>	0,033	0,028	0,061	0,055	0,036	0,027	0,09	0,079
<b>Total Q Losses (Mvar)</b>	0,224	0,191	0,271	0,247	0,186	0,142	0,264	0,237

From the results it is possible to see the settings adopted relating to the generation strategy. In this case it was assumed that the wind turbine never inputs reactive power, but only the maximum nominal active power. Obviously, the wind turbine will not always be out of service or at full power. However, the aim was to analyse the limit cases of generation.



As desired, in case of average load in connected-mode operation, the battery only feeds reactive power into the grid, to improve voltage quality at the nodes. In connected-mode operation and maximum load, the BESS sends approximately 0.37 MW as set, relieving the external grid of the task of covering demand peaks. When active, since the external source is the slack generator of the network, its reactive and active powers will be equal to the difference between the sum of the loads and losses minus the generation of the BESS and the wind turbine. In islanded mode, the BESS will work as the reference machine and therefore it will cover the power mismatch.

The load values take on only two values: one relating to the maximum load and one to the average load. In both cases, a power factor of 0.98 was assumed for all loads downstream of the network, while the auxiliary load relating to the BESS only requires active power.

The total active and reactive losses of the system are one of the most important results to analyse once a load flow analysis has been performed. Regarding active losses, the results coincide with expectations. The losses are directly proportional to the power demand values. In the case of distributed generation, losses decrease, as the distance that the power flow must travel from generation to load has been reduced. In this regard, note the difference between cases 8 and 4, between cases 7 and 3, between cases 6 and 2 and between cases 5 and 1. In these pairs of operational scenarios reported, the only difference is the possible presence of the DER. It can be noted that in these pairs the active losses are always lower in cases of active wind generation.

Regarding the item “reactive losses”, it is good to make a premise: it includes both the actual reactive losses and the power injected to improve the voltage of the power system. Since reactive power value of zero has been set for the turbine, the reactive losses do not depend on wind generation. Regardless of the operation of the wind turbine, the reactive power will always reach the loads from the 11 kV busbar. Obviously, here too the losses are greater in cases of maximum load.

Case 8 is the case where the BESS is called upon to do the greatest work. With the battery fully charged, assuming a minimum SOC (State of Charge) of 20% and having a nominal capacity of 3MVAh, the available capacity will be:  $C_n - SOC_{min}C_n = 2,4 \text{ MVAh}$ . Having  $P_{BESS} = 1,929 \text{ MW}$  and  $Q_{BESS} = 0,597 \text{ Mvar}$ , the apparent power injected in case 8 is by the BESS is  $\sqrt{(1,929^2 + 0,597^2)} = 2.02 \text{ MVA}$ . This means that, if the battery is fully charged before the fault occurs in the main grid, the microgrid can work in the worst case load in islanded mode for approximately 1.2 hours.

Table 6.4 Network Voltage Values in per unit.

	Case 1	Case 2	Case 3	Case 4	Case 5	Case 6	Case 7	Case 8
	(1-Co-AL-WG)	(2-Di-AL-WG)	(3-Co-ML-WG)	(4-Di-ML-WG)	(5-Co-AL-No WG)	(6-Di-AL-No WG)	(7-Co-ML-No WG)	(8-Di-ML-No WG)
33 kV Busbar	1,02	0	1,02	0	1,02	0	1,02	0
Battery Busbar	1,02	1,02	1,02	1,02	1,02	1,02	1,02	1,02
11 kV Busbar	1,01	1,01	1,01	1,01	1,01	1,01	1,01	1,01
Node EDN 2	1,02	1,02	1,01	1	1	1	0,98	0,98
busbar 2.1	1,03	1,01	1,01	1	0,99	0,99	0,97	0,96
Node EDN 2_1_2	1,03	1,03	1,01	1	0	0	0	0
Node EDN 2_1_1	1,02	1,02	1	1	0,99	0,98	0,96	0,96
Node EDN 2_2_1	1,02	1,01	1	1	1	0,99	0,98	0,97
Node EDN 2_2_2	1,02	1,01	1	0,99	0,99	0,99	0,98	0,97
Node EDN 1	1,01	1,01	1,01	1,01	1,01	1,01	1,01	1,01
Node EDN 1_1_1	0,99	0,99	0,97	0,97	0,99	0,99	0,97	0,97
Node EDN 1_2_1	0,99	0,99	0,98	0,97	0,99	0,99	0,97	0,97
Node EDN 1_1_2	0,99	0,98	0,96	0,96	0,99	0,98	0,96	0,96
Node EDN 1_2_2	0,99	0,99	0,97	0,97	0,99	0,99	0,97	0,97

Despite in certain cases the voltage of the nodes near the loads have undesirable and relatively low values, no voltage takes on values lower than 0,95 per unit, which is the minimum allowable value set, while the maximum value is 1,05 per unit.

It can be noted that the voltage values of the 33 kV busbar (unless the external network is disconnected), the battery busbar and the 11 kV one have the same values in per units for all cases: while for the first two this occurs at the discretion of the user, having directly set these desired per unit values, at the 11 kV busbar this occurs because the only voltage drops that occur upstream are related to the transformers. These losses are in no way comparable to the losses that occur in power lines.

For the same distributed generation and load conditions, it can be noted that the operating mode of the microgrid has a minimal influence on the general voltage of the nodes. This means that the battery is able to guarantee approximately the same quality of service offered by the national network, as desired.

The voltage values of the nodes downstream the node named EDN 1 (see figure 6.21) have similar voltage values to those downstream node EDN 2 when wind generation is out of service. On the contrary, in the case of operation of the wind turbine, the nodes downstream node EDN 1 enjoy only a minimal part of the positive effects of the wind turbine on node voltages, while the opposite can be said for all the nodes downstream EDN 2.

For cases 1 and 2, given the high per unit values, a target voltage for the battery and for the external source of 1,01 can be set, to see if the general trend of the node voltage tends better towards the nominal value of

1 per unit. In the other cases, the voltage values are generally lower: it is due to a greater load or the absence of wind generation. The wind turbine greatly helps the voltage quality of the nodes.

Table 6.5 shows the voltage values at the nodes for cases 1 and 2 by setting a voltage at the BESS and at the external grid of 1,01 per unit.

*Table 6.5 Network Voltage Values in per unit, Case 1 and 2 modified.*

	<b>Case 1</b>	<b>Case 2</b>
	<b>(1-Co-AL-WG)</b>	<b>(2-Di-AL-WG)</b>
<b>33 kV Busbar</b>	1,01	0
<b>Battery Busbar</b>	1,01	1,01
<b>11 kV Busbar</b>	1	1
<b>Node EDN 2</b>	1,01	1,01
<b>busbar 2.1</b>	1,02	1,02
<b>Node EDN 2_1_2</b>	1,02	1,02
<b>Node EDN 2_1_1</b>	1,02	1,01
<b>Node EDN 2_2_1</b>	1,01	1
<b>Node EDN 2_2_2</b>	1,01	1
<b>Node EDN 1</b>	1	1
<b>Node EDN 1_1_1</b>	0,98	0,98
<b>Node EDN 1_2_1</b>	0,98	0,98
<b>Node EDN 1_1_2</b>	0,98	0,97
<b>Node EDN 1_2_2</b>	0,98	0,98

As can be seen from the table, the voltage value set at the two power sources is a good alternative to the one initially hypothesized. This is a classic example of how load-flow analyses can be exploited to analyse the network and therefore improve the setting of operational parameters.

*Table 6.6 Power Line Loadings.*

<b>Loadings (%)</b>	<b>Case 1</b>	<b>Case 2</b>	<b>Case 3</b>	<b>Case 4</b>	<b>Case 5</b>	<b>Case 6</b>	<b>Case 7</b>	<b>Case 8</b>
	<b>(1-Co-AL-WG)</b>	<b>(2-Di-AL-WG)</b>	<b>(3-Co-ML-WG)</b>	<b>(4-Di-ML-WG)</b>	<b>(5-Co-AL-No WG)</b>	<b>(6-Di-AL-No WG)</b>	<b>(7-Co-ML-No WG)</b>	<b>(8-Di-ML-No WG)</b>
<b>L1</b>	13,5	13,5	24,4	24,5	13,5	13,5	24,4	24,5
<b>L2</b>	15,3	15,4	11,8	11,8	18,2	18,5	32,7	32,8
<b>L2_1</b>	6,1	6,1	11,5	11,6	13,6	13,6	24,6	24,7
<b>L2_2</b>	18	18,1	10,5	10,6	6,2	6,2	10,8	10,8
<b>L1_1</b>	32,8	32,9	59,7	60	32,9	32,9	58,8	60
<b>L1_2</b>	11,7	11,7	20,7	20,8	11,7	11,7	20,7	20,8

In Table 6.6 it is possible to see the load values of the power lines of the equivalent network. The L2\_2 line is generally the least stressed, while the one with the highest percentage of load is L1\_1. These two lines supply the smaller and the larger load of the series respectively. From the graph it is easy to see how the load percentage depends greatly on the load condition being studied. It can be seen how the branches of feeder 1 (L1) and Line L2\_2 are not affected by the presence of distributed generation, while for the L2\_1 branch the load changes according to the wind power generated. This is because if for the former the power flows come from the same nodes no matter the presence of distributed generation, in the case of wind generation the entire demand of the second load is satisfied directly by the wind turbine, without stressing the line L2\_1. Here too, no particular load variations are seen depending on the operating conditions of the microgrid.

# Chapter 7: Short-Circuit Analysis

## 7.1 Short-Circuit Analysis Theory

Short-circuit calculation is equally as important as load-flow calculations. It is used to understand how the system would behave in case of fault conditions. It is a method useful to verify if the protections the system would be equipped with could detect and withstand the fault, clearing it as soon as possible. In network planning, short-circuit calculations are fundamental not just for design and parametrization of protection, but could be used also to correctly dimension the earthing system and to check the thermal short-circuit capacity of cables. By means of softwares, it is possible to simulate both balanced and unbalanced faults.

This type of analysis is not only used for network planning purposes, but it could be useful also for operative power systems. For example, during network switching, this method can be used to verify if the operation is compliant with all the limits and therefore, if the system is working as planned. It could be also used to verify the actual tripping of protections, checking for possible protection maloperation and false tripping.

PowerFactory offers different short-circuit analysis method. Each of the methods available on PowerFactory are steady-state calculations. Despite this, by calculating some relevant characteristics of the short-circuit phenomenon, these methods offer a clear view of the transient under study (Fig.7.1) [21]:

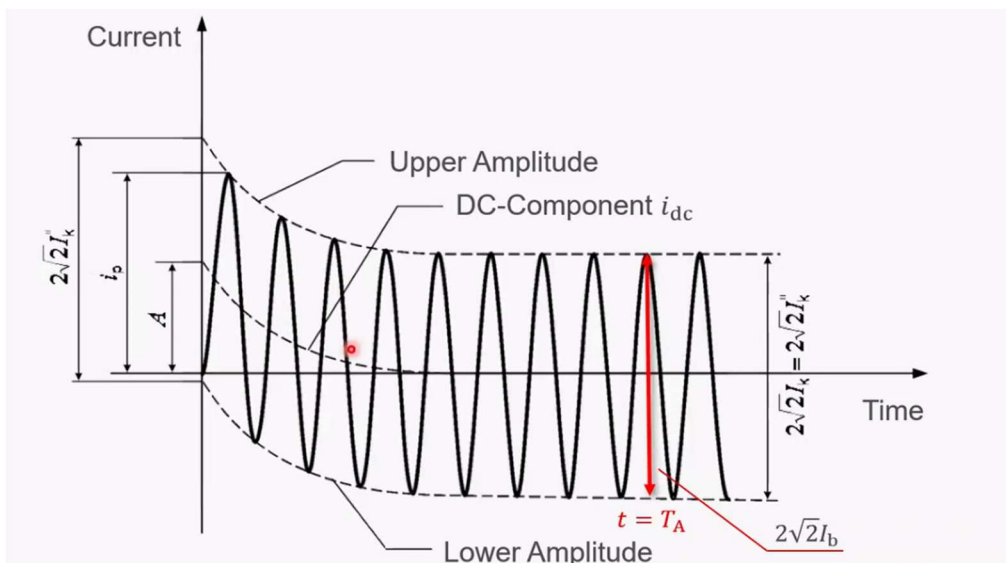


Fig. 7.1 Short-circuit Transient. [21]

In fact, through the short-circuit calculation, the software can record the initial peak short-circuit current  $i_p$ , the upper and the lower amplitude of the current during the transient phase, the steady-state short-circuit current, that is the current flowing in the fault after the transient phenomena stabilize, and the breaking current  $i_b$ , that is the current flowing in the circuit after a clearing time that must be set. This parameter is fundamental in breakers dimensioning. Depending on the distance of the fault to the generators in the network, the magnitude of the short-circuit current may or may not vary over time. If there are generators in

the proximity of the fault, the transient inductive effects of generation lead to an amplitude of the short-circuit current that varies over time. Otherwise, the inductive effects of generation are negligible and the amplitude of the short-circuit current does not depend on the time [29].

IEC is a simplified conservative short-circuit method used mostly in planning condition. It does not need to know the load-flow conditions of the network and therefore it works using a reduced set of data.

By imposing an equivalent voltage source at the fault location, it evaluates the sub-transient current  $I_{kss}$  and therefore it calculates the peak current  $I_p$ , the breaking current  $I_b$  and the thermal current  $I_{th}$ . The thermal current is used to determine the thermal stress on cables.

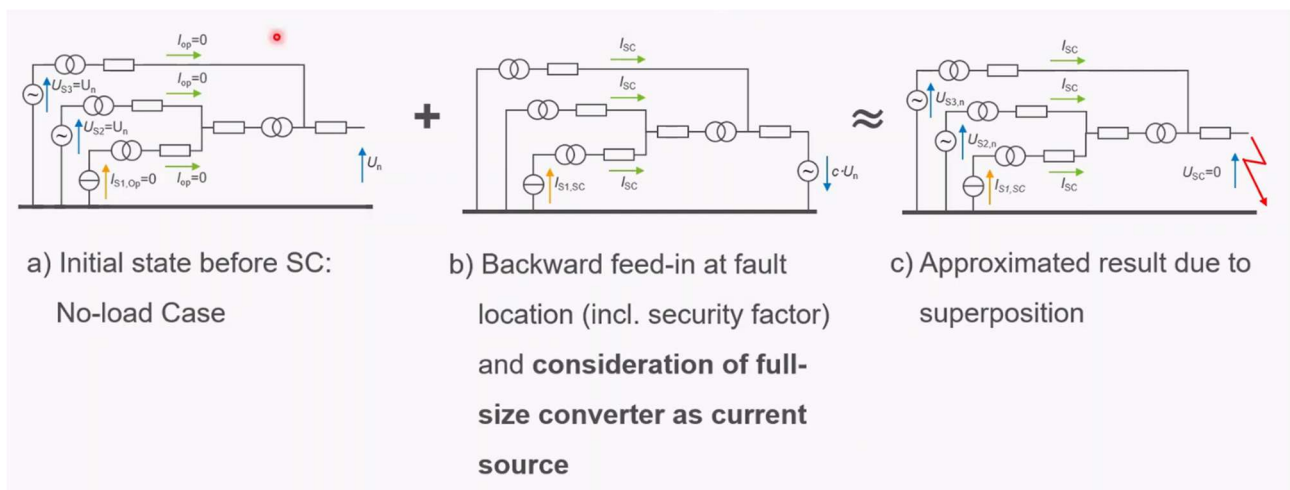


Fig 7.2 IEC Superimposition Method. [29]

As indicated in Fig. 7.2, the approximated result of the IEC method is the superposition of two different models:

The first one represents the no-load case, in which the voltage of each generator is equal to the nominal voltage in the fault location. In the second model a voltage source with opposite sign is represented in the fault location. A c-factor (correction factor) is used for security issues: defining a c-factor higher than one makes the short-circuit current results more conservative. In this model currents flow from the generators.

The results of the analysis will be more conservative as the value of the c-factor increases. Within the software it is possible to set a maximum and minimum c-factor value, from which respectively the maximum and minimum sub-transient current is evaluated.

Fig. 7.3 shows a table from standards of typical maximum and minimum correction factors according to the nominal voltage.

### Voltage Correction Factors:

Nominal Voltage	Calc. max. SC Current	Calc. min. SC Current
	$c_{max}$	$c_{min}$
Low Voltage $U_n \leq 1 \text{ kV}$	1.05 (for $U_{max} \leq 1.06 \cdot U_n$ ) 1.10 (for $U_{max} \leq 1.10 \cdot U_n$ )	0.95 (for $U_{max} \leq 1.06 \cdot U_n$ ) 0.9 (for $U_{max} \leq 1.10 \cdot U_n$ )
High Voltage $1 \text{ kV} < U_n \leq 230 \text{ kV}$	1.10	1.00
High Voltage $230 \text{ kV} < U_n < 420 \text{ kV}$	1.10 If $U_n$ not defined: $c_{max} \cdot U_n \rightarrow U_m$	1.00 If $U_n$ not defined: $c_{min} \cdot U_n \rightarrow 0.9 \cdot U_m$

Fig. 7.3 Voltage Correction Factors. [29]

Another method that can be used in Powerfactory is the Complete Method. It is a more accurate steady-state method which takes into account the load conditions of the system. As the IEC method, the complete method determines  $I_p$ ,  $I_b$  and  $I_{th}$  once it evaluates the sub-transient current  $i_{kss}$ .

As clear from Fig. 7.4, the superposition method used is similar to the one shown for IEC 60909. The main difference is the initial state before the short-circuit: while the IEC 60909 assumes a no-load state, the complete method assumes as the initial state the one calculated by means of a load-flow analysis.

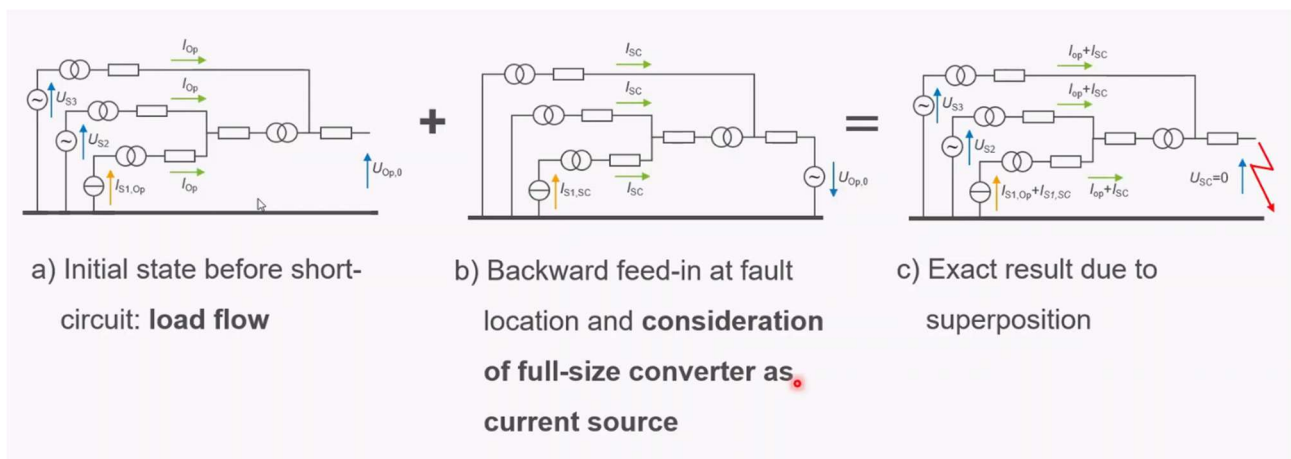


Fig. 7.4 Superimposition Complete Method. [29]

The formula coming from standards regarding the thermal current evaluation is the following:

$$\int_0^{T_k} i^2 dt = I_k''^2 (m + n) T_k = I_{th}^2 T_k \rightarrow I_{th} = I_k'' \sqrt{(n + m)} \quad (7.1)$$

where:

- $T_k$  is the fault duration
- $i$  is the current flowing in the fault
- $I_k''$  is the sub-transient short-circuit current ( $I_{kss}$ )
- $m$  and  $n$  are factors for heating effect, dependent on frequency,  $\kappa$  and  $T_k$
- $I_{th}$  is the thermal current.

Talking about the peak power  $i_p$ :

$$i_p = \kappa \sqrt{2} I_k'' \quad (7.2) \quad \text{with } \kappa = 1,02 + 0,98 e^{-3R/X} \quad (7.3)$$

Observing the formula, it is possible to see that the higher the  $R/X$  ratio, the lower the  $\kappa$ -factor.



## 7.2 Component Setting for Short-Circuit Analysis

In the theoretical chapter of short-circuit analysis, the complete method and the IEC 60909 method have been exposed. While the latter is used in the network design phase, the complete method is more accurate, given that it considers also information relating to loads. The complete method will be used to carry out the analysis, as it is more compliant with the study in question.

The study will limit itself to commenting and comparing the results of the characteristic currents of the short-circuit transient of the eight operation scenarios previously analysed in the load-flow analysis. Only three-phase faults have been simulated.

Before analysing the results, the settings for the analysis are exposed both for the short-circuit command, through which the analysis is performed, and for the network components. For some components, such as nodes and busbars, there is no need to add additional data to perform the analysis. Since it is assumed that the loads do not contribute to the fault, their pages relative to the complete method are not shown. Moreover, there is no need to enter any other data relating to terminals and earthing connections.

### 7.2.1 External Grid

Max. Values		Min. Values	
Short-Circuit Power $S_k^{\text{max}}$	1428,942 MVA	Short-Circuit Power $S_k^{\text{min}}$	1428,885 MVA
Short-Circuit Current $I_k^{\text{max}}$	25, kA	Short-Circuit Current $I_k^{\text{min}}$	24,999 kA
c-Factor (max.)	1,01	c-Factor (min.)	1,
R/X Ratio (max.)	0,2	R/X Ratio (min.)	0,2
Impedance Ratio		Impedance Ratio	
Z2/Z1 max.	1,	Z2/Z1 min.	1,
X0/X1 max.	1,	X0/X1 min.	1,
R0/X0 max.	0,1	R0/X0 min.	0,1

Fig. 7.5 External Grid Complete Method Data.

Fig. 7.5 shows the dialog box relating to the complete method of the external source. To have a unique result, the maximum and minimum values will purposely differ slightly. It is known that the short-circuit current coming from the external source is equal to 25 kA [19]. the short-circuit power will be automatically calculated by the software through the equation:  $S^{k''} = \sqrt{3}U_n I^{k''}$ .

Having chosen the complete method for the short-circuit analysis and knowing the load values of the limit cases to analyse, it is entered a c-factor values tending to one.

The  $R/X$  ratio depends on the technical-physical characteristics of the upstream network. Not having such data available, the  $R/X$  ratio is assumed by knowing that the distribution network downstream the substation

is very resistive. For this reason, it is believed that an  $R/X$  ratio of 0,2 may be a likely value to proceed with the study.

The relationships between impedances, resistances and reactances of positive sequence 1, negative 2 and zero sequence 0 are not necessary data for the analysis, given that only the three-phase faults will be treated, the only data necessary are those relating to the positive sequence. These ratio values will be left the same as the default ones.

## 7.2.2 Transformers

As seen in the network modeling part and in the load-flow analysis, to fully describe the transformers it is necessary to define the transformer Type and the transformer Element.

As for the transformer Element, the only thing that needs to be specified is the tap position before starting the analysis. Inside the transformer Object, however, two pages must be defined:

- one relating to the tap changer, where the number of positions that the tap can fill and the additional voltage per tap are defined.
- a general page, where it is possible to enter the values of no-load current, no-load losses and the distribution of leakage reactances and resistances.

While the data of the 33/11 kV transformer and the battery transformer are known almost entirely, this is not true for the transformers present downstream the equivalent network. This is because these transformers are not real, but have been modeled and sized based on the demands of the low voltage loads. Consequently, the values of no-load current and no-load losses will be taken from the datasheets of transformers having dimensions similar to those of the load transformers [26]. An equal distribution of leakage reactances and resistances is assumed between the primary and secondary windings of the transformers.

All the parameters just mentioned were previously entered in the load-flow and basic data pages. For this reason, the exposure of the figures is omitted.

## 7.2.3 Lines

The only page to fill regarding the short-circuit analyses of the line component lies in the line Object. For all the lines present in the model, a maximum operating temperature of 80° C is assumed, equal to the maximum temperature of the real cables from which the equivalent network was taken. The AC-Resistance at 20°C is the one obtained in the study of the equivalent model. In the short-circuit analysis, the resistances at the maximum operating temperature come into play. It is known that the cables are all underground, made of copper, with PVC as insulation. Through the temperature coefficient relating to the type of conductor, the software automatically calculates the resistance at maximum temperatures. As mentioned in the modeling of the equivalent network, the capacitive components and the insulation factor of the cables are set equal to zero.

All the data necessary to carry out the analysis have already been shown in the equivalent network modeling chapter, consequently only the complete method page relating to a line is exposed.

The screenshot shows a software interface for configuring line parameters. It is organized into four main sections:

- Parameters per Length 1,2-Sequence (Top-Left):**
  - Max. End Temperature: 80, degC
  - AC-Resistance R'(20°C): 0,75 Ohm/km (with a gear icon)
  - Conductor Material: Copper (dropdown menu)
- Parameters per Length 1,2-Sequence (Bottom-Left):**
  - Capacitance C': 0, uF/km (with a gear icon)
  - Ins. Factor: 0, (with a gear icon)
- Parameters per Length Zero Sequence (Top-Right):**
  - Capacitance C0': 0, uF/km (with a gear icon)
- Parameters per Length Zero Sequence (Bottom-Right):**
  - Ins. Factor: 0, (with a gear icon)

Fig. 7.6 Line Type Complete Method Data.

## 7.2.4 BESS

Depending on the type of static generator, there are a series of short-circuit models that may be most suitable for a component. Among these models, the best to represent BESS is the Full-Size Converter short-circuit model.

To express the contribution to the battery failure, the software uses a piecewise function. Fig. 7.7 is taken from the reference manual for static generators and includes both the piecewise function and the descriptions of the relevant parameters [22]:

The magnitude of the injected current,  $|\Delta I_1|$ , is calculated as follows:

$$\Delta u_1 = \frac{|\underline{U}_{1,tdf}| - |\underline{U}_{1,ros}|}{U_N}$$

$$|\Delta I_1| = \begin{cases} K \cdot \Delta u_1 \cdot I_N & \text{if } K \cdot \Delta u_1 < i_{max} \\ i_{max} \cdot I_N & \text{if } K \cdot \Delta u_1 \geq i_{max} \end{cases}$$

where:

- $i_{max}$  is the maximum current injection in p.u. (e:*imax*)
- $I_N$  is the nominal current in kA ( $I_N = S_N / (\sqrt{3} \cdot U_N)$ )
- $S_N$  is the nominal apparent power in MVA (e:*sgn*)
- $U_N$  is the nominal voltage in kV (e:*uknom* of the connected bus)
- $\underline{U}_{1,tdf}$  is the positive sequence pre-fault voltage in kV
- $\underline{U}_{1,ros}$  is the retained positive sequence voltage from rotating machines in kV
- $K$  is a scaling factor (e:*K*)

Fig. 7.7 BESS SC Current Piecewise Function. [22]

From the piecewise function it is noted that if  $K\Delta u_1 > i_{max}$  then the short-circuit current injected  $\Delta I_1$  into the network is equal to the product between the rated current  $I_N$  of the BESS and the parameter  $i_{max}$ , which describes the ratio between the short-circuit current and the rated current. It is desired to define the short-circuit current within the software through the  $i_{max}$  value, known from the technical specifications and equal to 2 per unit. For this reason, an arbitrary and high value is attributed to the scaling factor  $K$ , to comply with the condition  $K\Delta u_1 > i_{max}$ .

No voltage deadband is considered in the analysis. The default values for the negative sequence short-circuit impedance values are retained.

The screenshot displays a software interface for configuring a BESS (Battery Energy Storage System) model. The 'Short-Circuit Model' is set to 'Full size converter'. There is an unchecked checkbox for 'Externally modelled unit transformer'. The 'Fault Contribution' section includes a gear icon for settings. The 'K Factor' is set to '10,' and the 'Max. Current' is set to '2,' p.u. The 'Voltage deadband' section has three radio button options: 'No deadband' (selected), 'From pre-fault voltage', and 'From nominal voltage'.

Fig 7.8 BESS Complete Method Page

## 7.2.5 Wind Turbine

Since wind generation is also represented through a static generator, there is a need to adopt the more accurate short-circuit model. Not knowing the type of turbine generator, it is assumed that it is of the synchronous type. For this the equivalent synchronous machine short-circuit model has been chosen.

The precise choice of these parameters is complicated, and it has been made taking into consideration the documentation available relating to the technology in question [30]. Having a nominal current of approximately 1 kA, it is assumed a sub-transient short-circuit current and a transient short-circuit current respectively seven and four times greater than the nominal value. Finally, a plausible ratio value between reactance and resistance in the sub-transient domain of 2,5 is entered [31].

The default values for the negative sequence short-circuit impedance values are retained, since they are not of interest to the analysis.

Short-Circuit Model Equivalent synchronous machine

Fault Contribution ⚙️

Subtransient Short-Circuit Current 7,  kA

Transient Short-Circuit Current 4,  kA

X'' to R ratio 5,

Negative sequence short-circuit impedance

Resistance, r2 99999,  p.u.

Reactance, x2 99999,  p.u.

Fig 7.9 Wind Turbine Complete Method Page.

## 7.3 Short-Circuit Command Settings

The screenshot shows the 'Basic Options' page of a software interface for configuring a short-circuit command. On the left, there is a vertical navigation menu with four items: 'Basic Options' (selected), 'Advanced Options', 'Output', and 'Verification'. The main area contains several configuration sections:

- Method:** A dropdown menu set to 'complete'. To its right, a green note reads: 'Select 'complete' method to calculate multiple faults.'
- Fault Type:** A dropdown menu set to '3-Phase Short-Circuit'. Below it is an unchecked checkbox labeled 'Multiple Faults'.
- Calculate:** A dropdown menu set to 'Max. Short-Circuit Currents'.
- Load Flow:** A button with a right-pointing arrow and the text 'Study Cases\Power Flow\Load Flow Calculation'.
- Short-Circuit Duration:** A sub-section containing:
  - Break Time:** A text input field with '0,1' and a unit 's'.
  - Used Break Time:** A dropdown menu set to 'global'.
  - Fault Clearing Time (Ith):** A text input field with '1,' and a unit 's'.
- Fault Impedance:** A sub-section containing:
  - An unchecked checkbox labeled 'Enhanced Fault Impedance Definition'.
  - Resistance, Rf:** A text input field with '0,' and a unit 'Ohm'.
  - Reactance, Xf:** A text input field with '0,' and a unit 'Ohm'.
- Fault Location:** A sub-section containing:
  - At:** A dropdown menu set to 'Busbars and Junction Nodes'.

On the right side of the dialog, there are four buttons: 'Execute' (highlighted in blue), 'Close', 'Cancel', and 'Contents'.

Fig. 7.10 Basic Options, Short-Circuit Command.

As clear from figure 7.10, the short-circuit command is divided into four pages: the Basic Options, Advanced Options, Output and Verification page.

In the Basic Data page it is possible to choose the short-circuit method and the fault type. As said previously, the method used is the complete short-circuit method and the 3-Phase short-circuit fault will be investigated. It is possible to choose between the maximum and minimum short-circuit current results, according to the minimum and maximum c-factors adopted: since these parameters has been set almost equal one to another, the results will be the same no matter the c-factor adopted.

Regarding the short-circuit duration, a break time of 100 ms and a fault clearing time of 1 second has been set. The more the fault is exposed to short-circuit phenomena, the more the network component will be degraded.

It has been chosen to set the resistance and reactance values equal to zero: this is a conservative choice, given that as the impedance of the fault increases, the short-circuit currents decrease.

The software gives the possibility to enter three different types of fault locations:

1. All busbars
2. Busbars and junction nodes
3. User selection: in this case it is possible to choose manually the fault location

In this case the short-circuit current will be evaluated for all the busbar and junction nodes.

Fig. 7.11 Advanced Options, Short-Circuit Command.

Fig. 7.11 shows the Advanced Option page. In this page it is possible to customize the command in detail. As can be seen from the top left of the figure, it is possible to choose between different methods. It is not wanted to go into detail about how each method works and the  $C(1)$  method is used. For the rest of the page the default settings are used: the analysis is initialized from the load-flow condition in the instant before the fault and the currents of the transient and sub-transient phase is calculated. Since the purpose of the study does not concern the analysis of protection and their functioning, the settings relating to them are not discussed.

The Output page is used if the user wants to show the results also in the output window.

Regarding the Verification page, quoting the user manual, “When enabled, the user can enter thresholds for peak, interrupting and thermal maximum loading. The Verification option will then write a loading report to the output window with all devices that have higher loadings than the defined maximum values. This report shows the various maximum and calculated currents for rated devices.” [21].



## 7.4 Short-Circuit Analysis Results

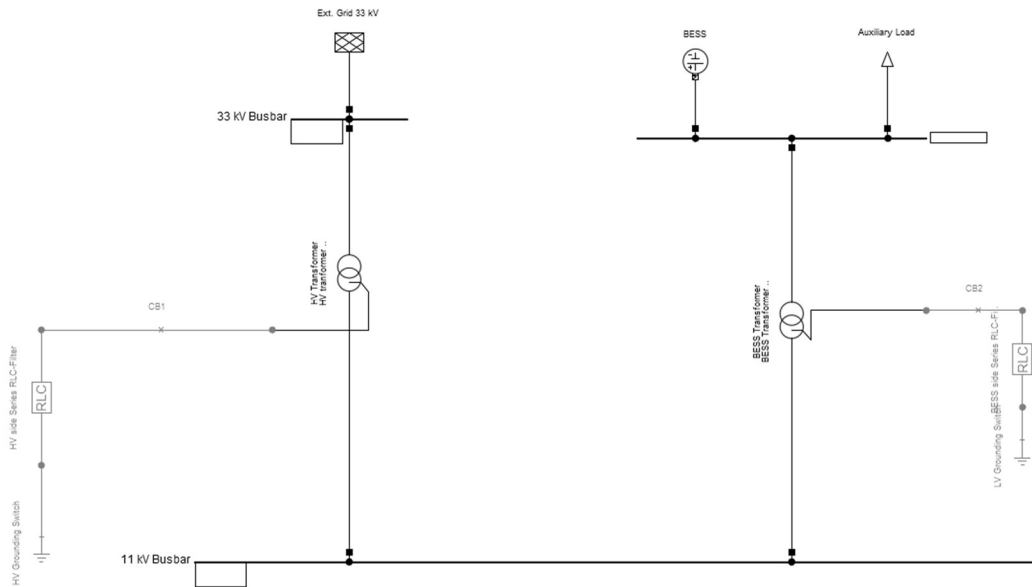


Fig. 7.12 Drynoch primary substation model.

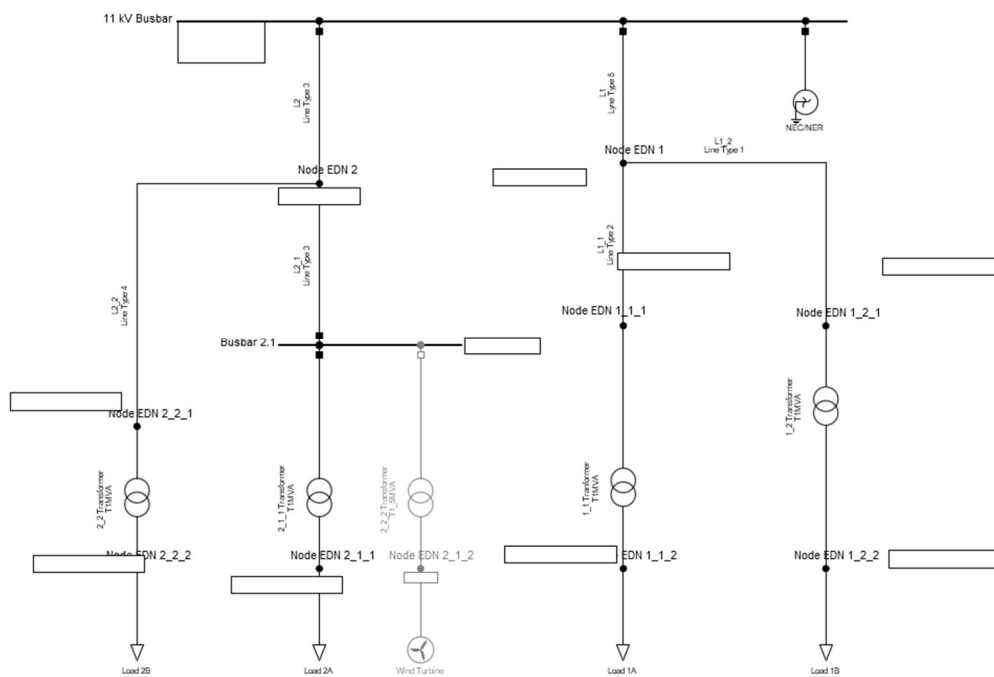


Fig. 7.13 Equivalent Distribution Network Model.

In this chapter the results of the short-circuit analysis are presented. As mentioned in the theoretical introductory part of the analysis, through the complete method used for the study, the software first calculates the initial sub-transient short-circuit current  $I_{kss}$ . From this parameter, it evaluates the peak current

in the sub-transient phase  $i_p$ , the breaking current  $i_b$ , which is the short-circuit current calculated at the breaking time and the thermal current  $i_{th}$ , a useful parameter for understanding the level of damage that the faulty component suffers.

The values obtained are analysed in detail, comparing the results of the limit cases analysed previously in the load-flow analysis chapter. The different case studies are exposed again, with their own characteristics and codes:

- Case 1: Connected grid, Average load, Wind generation (1-Co-AL-WG)
- Case 2: Disconnected grid, Average load, Wind generation (2-Di-AL-WG)
- Case 3: Connected grid, Maximum load, Wind generation (3-Co-ML-WG)
- Case 4: disconnected grid, maximum load, wind generation (4-Di-ML-WG)
- Case 5: connected grid, average load, no wind generation (5-Co-AL-No WG)
- Case 6: disconnected grid, average load, no wind generation (6-Di-AL-No WG)
- Case 7: connected grid, maximum load, no wind generation (7-Co-ML-No WG)
- Case 8: disconnected grid, maximum load, no wind generation (8-Di-ML-No WG)

Table 7.1 shows the initial short-circuit peak currents for all the nodes and operation scenarios analysed.

*Table 7.1 Short Circuit Peak Currents.*

$i_p$	Case 1	Case 2	Case 3	Case 4	Case 5	Case 6	Case 7	Case 8
	(1-Co-AL-WG)	(2-Di-AL-WG)	(3-Co-ML-WG)	(4-Di-ML-WG)	(5-Co-AL-No WG)	(6-Di-AL-No WG)	(7-Co-ML-No WG)	(8-Di-ML-No WG)
<b>33 kV Busbar</b>	49,74	0	49,74	0	49,66	0	49,67	0
<b>Battery Busbar</b>	36,51	8,97	36,37	8,86	35,31	5,44	35,19	5,44
<b>11 kV Busbar</b>	5,4	0,84	5,39	0,84	5,06	0,5	5,07	0,5
<b>Node EDN 2</b>	2	0,91	1,99	0,91	1,59	0,51	1,58	0,52
<b>busbar 2.1</b>	1,44	0,98	1,44	0,99	0,96	0,52	0,96	0,54
<b>Node EDN 2_1_2</b>	22,06	28,91	36,76	29,32	0	0	0	0
<b>Node EDN 2_1_1</b>	24,28	21,69	24,11	21,96	18,39	14,31	18,33	14,95
<b>Node EDN 2_2_1</b>	1,07	0,81	1,06	0,81	0,93	0,51	0,93	0,53
<b>Node EDN 2_2_2</b>	20,02	18,57	19,83	18,72	18,05	14,13	17,89	14m57
<b>Node EDN 1</b>	4,85	0,84	4,85	0,83	4,58	0,5	4,58	0,51
<b>Node EDN 1_1_1</b>	1,23	0,74	1,23	0,75	1,22	0,51	1,22	0,53
<b>Node EDN 1_2_1</b>	0,54	0,59	0,54	0,6	0,54	0,51	0,54	0,53
<b>Node EDN 1_1_2</b>	22,06	17,49	22,04	17,92	21,98	14,31	21,97	14,95
<b>Node EDN 1_2_2</b>	12,29	14,51	12,24	14,75	12,26	14,17	12,21	14,65

While for the battery busbar the same values were recorded for the different cases, the values for the 33 kV busbar depend on the connection with the external network.

The factor that most affects the amplitude of the currents on the 11 kV busbar is the operating state of the network: as can be seen from the Table 7.1, in fact, if the network is connected to the main network, much higher values of initial short-circuit peak currents are recorded.

The different contribution of wind generation on currents is evident from the analysis. Take cases 1 and 5 as example, which differ only in the state of the wind turbine. Note the difference in the values recorded in the two different cases for the EDN 2\_1\_1 node, close to the generation, and for the EDN 1\_2\_2 node, very far from the renewable source: it is evident that the presence of generation influences the first node much more than the second, for which the current values are on the contrary little disturbed by this factor.

The points with the highest recorded currents are the connection nodes of the equivalent loads. This condition is consistent with expectations, given that they are in a low voltage area. The amount of energy required by the loads does not influence the nature of the currents obtained from the analysis as much as the operating mode and the presence of wind generation. However, remember that it was assumed that the loads do not contribute to the fault.

Although it is not the purpose of the study, the complexity of protecting microgrids can be seen from the analysis: the coordination of protections and their calibrations strongly depend on the presence of distributed generation as well as on the operating mode of the microgrid. When these factors vary, there is a need to switch the protective strategy to be adopted, which is defined in accordance with the results of the analysis.

The breaking current and thermal current values are reported in Table 7.2 and Table 7.3 respectively. It is easy to see how they have the same pace as the initial peak of the short-circuit currents previously analysed.

*Table 7.2 Short Circuit Breaking Currents*

<i>I<sub>b</sub></i>	Case 1	Case 2	Case 3	Case 4	Case 5	Case 6	Case 7	Case 8
	(1-Co-AL-WG)	(2-Di-AL-WG)	(3-Co-ML-WG)	(4-Di-ML-WG)	(5-Co-AL-No WG)	(6-Di-AL-No WG)	(7-Co-ML-No WG)	(8-Di-ML-No WG)
<b>33 kV Busbar</b>	25,43	0	25,29	0	25,4	0	25,3	0
<b>Battery Busbar</b>	16,48	5,15	16,42	5,11	16,04	3,85	16	3,85
<b>11 kV Busbar</b>	2,37	0,48	2,37	0,48	2,25	0,35	2,25	0,36
<b>Node EDN 2</b>	1,15	0,48	1,14	0,49	1,02	0,36	1,02	0,37
<b>busbar 2.1</b>	0,76	0,49	0,76	0,5	0,64	0,37	0,64	0,38
<b>Node EDN 2_1_2</b>	17,41	11,15	17,31	11,49	0	0	0	0
<b>Node EDN 2_1_1</b>	11,81	11,55	11,74	11,82	10,94	10,12	10,9	10,57
<b>Node EDN 2_2_1</b>	0,69	0,46	0,69	0,47	0,63	0,36	0,63	0,37
<b>Node EDN 2_2_2</b>	11,53	11,1	11,42	11,27	10,96	9,99	10,87	10,31
<b>Node EDN 1</b>	2,26	0,48	2,26	0,48	2,15	0,35	2,15	0,36
<b>Node EDN 1_1_1</b>	0,85	0,46	0,85	0,47	0,84	0,36	0,84	0,38
<b>Node EDN 1_2_1</b>	0,38	0,41	0,37	0,42	0,37	0,36	0,37	0,37
<b>Node EDN 1_1_2</b>	13,33	11,15	13,31	11,49	13,24	10,12	13,23	10,57
<b>Node EDN 1_2_2</b>	8,32	10,06	8,29	10,27	8,29	10,02	8,25	10,36

Table 7.3 Short Circuit Thermal Currents.

<i>I</i> th	Case 1	Case 2	Case 3	Case 4	Case 5	Case 6	Case 7	Case 8
	(1-Co-AL-WG)	(2-Di-AL-WG)	(3-Co-ML-WG)	(4-Di-ML-WG)	(5-Co-AL-No-WG)	(6-Di-AL-No-WG)	(7-Co-ML-No-WG)	(8-Di-ML-No-WG)
<b>33 kV Busbar</b>	25,57	0	25,57	0	25,53	0	25,53	0
<b>Battery Busbar</b>	16,9	5,73	16,84	5,66	16,3	3,85	16,25	3,85
<b>11 kV Busbar</b>	2,45	0,54	2,45	0,54	2,28	0,35	2,28	0,36
<b>Node EDN 2</b>	1,22	0,56	1,21	0,56	1,02	0,36	1,02	0,37
<b>busbar 2.1</b>	0,84	0,57	0,84	0,58	0,64	0,37	0,64	0,38
<b>Node EDN 2_1_2</b>	20,25	11,38	20,15	16,97	0	0	0	0
<b>Node EDN 2_1_1</b>	12,38	12,44	12,29	12,65	10,97	10,12	10,93	10,57
<b>Node EDN 2_2_1</b>	0,72	0,5	0,71	0,53	0,63	0,36	0,63	0,37
<b>Node EDN 2_2_2</b>	11,79	11,55	11,68	11,67	10,99	9,99	10,9	10,31
<b>Node EDN 1</b>	2,32	0,54	2,32	0,53	2,17	0,35	2,17	0,36
<b>Node EDN 1_1_1</b>	0,85	0,49	0,85	0,5	0,84	0,36	0,84	0,38
<b>Node EDN 1_2_1</b>	0,38	0,4	0,37	0,41	0,37	0,36	0,37	0,37
<b>Node EDN 1_1_2</b>	13,38	11,38	13,37	11,68	12,28	10,12	13,27	10,57
<b>Node EDN 1_2_2</b>	8,33	9,76	8,3	9,93	8,3	10,02	8,27	10,36

Table 7.4 shows the amplitude of the initial short-circuit current  $I_{kss}$  in the sub-transient phase, while Table 7.5 shows the total amplitude in the transient phase  $I_{ks}$ . The closer the nodes are to the generation, the greater the difference in the reported currents. For example, note the currents of the EDN node 1\_2\_2, the furthest from the WG, and the node 2\_1\_1, very close to the WG. It can be noted that the difference between the  $I_{kss}$  and  $I_{ks}$  currents of the last node is much more significant than that found in the currents of the EDN 1\_2\_2 node.

*Table 7.4 Initial Short-Circuit Current.*

Ikss	Case 1	Case 2	Case 3	Case 4	Case 5	Case 6	Case 7	Case 8
	(1-Co-AL-WG)	(2-Di-AL-WG)	(3-Co-ML-WG)	(4-Di-ML-WG)	(5-Co-AL-No WG)	(6-Di-AL-No WG)	(7-Co-ML-No WG)	(8-Di-ML-No WG)
33 kV Busbar	25,44	0	25,44	0	25,29	0	25,4	0
Battery Busbar	16,65	5,7	16,59	5,84	16,04	3,85	16	3,85
11 kV Busbar	2,42	0,54	2,42	0,53	2,25	0,35	2,25	0,36
Node EDN 2	1,22	0,55	1,21	0,56	1,02	0,36	1,02	0,37
busbar 2.1	0,84	0,57	0,83	0,58	0,64	0,37	0,64	0,38
Node EDN 2_1_2	20,17	16,54	20,06	16,83	0	0	0	0
Node EDN 2_1_1	12,31	12,35	12,22	12,57	10,94	10,12	10,9	10,57
Node EDN 2_2_1	0,72	0,51	0,71	0,52	0,63	0,36	0,63	0,37
Node EDN 2_2_2	11,75	11,52	11,64	11,64	10,96	9,99	10,87	10,31
Node EDN 1	2,3	0,53	2,3	0,53	2,15	0,35	2,15	0,36
Node EDN 1_1_1	0,85	0,49	0,84	0,5	0,84	0,36	0,84	0,38
Node EDN 1_2_1	0,37	0,4	0,37	0,41	0,37	0,36	0,37	0,37
Node EDN 1_1_2	13,34	11,36	11,33	11,66	13,24	10,12	13,23	10,57
Node EDN 1_2_2	8,32	9,75	8,29	9,92	8,29	10,12	8,25	10,36

Table 7.5 Short-Circuit Current in the Transient Phase

<i>I<sub>ks</sub></i>	Case 1	Case 2	Case 3	Case 4	Case 5	Case 6	Case 7	Case 8
	(1-Co-AL-WG)	(2-Di-AL-WG)	(3-Co-ML-WG)	(4-Di-ML-WG)	(5-Co-AL-No WG)	(6-Di-AL-No WG)	(7-Co-ML-No WG)	(8-Di-ML-No WG)
33 kV Busbar	25,29	0	25,29	0	25,29	0	25,3	0
Battery Busbar	16,46	5,1	16,41	5,06	16,04	3,85	16	3,85
11 kV Busbar	2,37	0,47	2,37	0,47	2,25	0,35	2,25	0,36
Node EDN 2	1,14	0,48	1,14	0,48	1,02	0,36	1,02	0,37
busbar 2.1	0,74	0,48	0,75	0,49	0,64	0,37	0,64	0,38
Node EDN 2_1_2	17,16	13,54	17,06	13,83	0	0	0	0
Node EDN 2_1_1	11,76	11,42	11,69	11,68	10,94	10,12	10,9	10,57
Node EDN 2_2_1	0,69	0,46	0,68	0,47	0,63	0,36	0,63	0,37
Node EDN 2_2_2	11,5	11	11,4	11,16	10,96	9,99	10,87	10,31
Node EDN 1	2,25	0,47	2,25	0,47	2,15	0,35	2,15	0,36
Node EDN 1_1_1	0,85	0,45	0,85	0,47	0,84	0,36	0,84	0,38
Node EDN 1_2_1	0,38	0,4	0,37	0,41	0,37	0,36	0,37	0,37
Node EDN 1_1_2	13,32	11,07	13,31	11,41	13,24	10,12	13,23	10,57
Node EDN 1_2_2	8,32	10	8,28	10,21	8,29	10,02	8,25	10,36



# Conclusions

The aim of the thesis was to thoroughly analyse the performance of an electricity network on the Isle of Skye, Scotland. In particular, the scope was to observe the behavior and critical issues of the network once a lithium-ion battery storage system was integrated into the Drynoch primary substation, enabling the downstream portion of the network to operate in islanded mode.

Using the PowerFactory software, an equivalent network was then modeled that represented the real network as faithfully as possible. Following this, two separate analyses have been carried out: the load-flow analysis and the short-circuit analysis.

Eight different limit operation scenarios were analysed, depending on the type of network operation mode, the value of demand and the possible presence of distributed generation:

- Case 1: Connected grid, Average load, Wind Generation
- Case 2: Disconnected grid, Average load, Wind Generation
- Case 3: Connected grid, Maximum load, Wind Generation
- Case 4: Disconnected grid, Maximum load, Wind Generation
- Case 5: Connected grid, Average load, No Wind Generation
- Case 6: Disconnected grid, Average load, No Wind Generation
- Case 7: Connected grid, Maximum load, No Wind Generation
- Case 8: Disconnected grid, Maximum load, No Wind Generation

The BESS has been set up in such a way as to always provide reactive power to the grid. In the case of a microgrid connected to the main grid, the BESS inputs active power only to cover peaks in demand, while in the case of working in islanded mode, it cooperated with distributed generation to satisfy the demand.

The voltage at the loads depends more on the type of load (average or maximum) and on the power injected by the DER than on the mode of operation of the network. It is therefore concluded that without any faults in the microgrid the islanded mode system guarantees the same voltage quality of service offered in connected mode.

From the results obtained, the usefulness of the DER on the voltage quality in the nodes further downstream the network can be seen. In fact, its presence causes the voltage of the nodes to tend to the optimal value. This is very beneficial for the type of network analysed; in fact, without the DER generation the voltage values at loads are typical of remote and rural electricity networks.

Once an anomaly has been detected in the main network, the BESS with the maximum SOC, in the absence of wind generation and in the case of maximum load, is able to supply the network on its own for approximately 1,2 hours.

Even in the worst-case scenario, the power line loadings never assume values higher than 60%. In these terms, the lines are more than suitable for power transfer and can support greater loads in the future.

In the part relating to the short-circuit analysis, the same limit operational scenarios were analysed. For each of them, a three-phase node fault analysis was carried out using the complete method available on



PowerFactory. For the purposes of the study, it has been chosen to use a c-factor of one. The analysis reported all the characteristic current values of the transient and the thermal current.

It is concluded that the fault currents at each node of the system differ considerably depending on the operation mode. In fact, in the case of grid-tied operation these currents are much higher than those found in islanded mode. For this reason, the network is to be considered weaker in islanded mode, given that lower short-circuit currents imply greater voltage variations in the event of a fault.

It is clear from the results that the influence of the short-circuit power of the wind generation on the short-circuit currents of the nodes decreases as a function of the distance of the nodes themselves.

It is easy to see from the results that ensuring network protection for this type of networks is a much more complex task than ensuring it for conventional centralized networks. The type of protection, its calibration and the protections coordination vary depending on the operating mode of the network.

This research could be expanded on several fronts. In fact, it would be interesting to carry out a similar type of study for the load values expected in the immediate future, or a dynamic study to define the optimal battery management strategy that guarantees a consistent voltage quality service but at the same time guarantees a certain quantity of minimum energy in case of anomalies in the main network and therefore of switches in islanded mode. Finally, the research could be expanded by looking in detail at the challenges of designing an adequate protection system for the network.



# Bibliography

- [1] “Climate Change: Atmospheric Carbon Dioxide | NOAA Climate.gov.” [Online]. Available: <https://www.climate.gov/news-features/understanding-climate/climate-change-atmospheric-carbon-dioxide>
- [2] “Emissioni di gas serra per paese e settore: Infografica | Attualità | Parlamento europeo [Online]. Available: [https://www.europarl.europa.eu/news/it/headlines/society/20180301STO98928/emissioni-di-gas-serra-per-paese-e-settore-infografica?at\\_campaign=20234-](https://www.europarl.europa.eu/news/it/headlines/society/20180301STO98928/emissioni-di-gas-serra-per-paese-e-settore-infografica?at_campaign=20234-)
- [3] “World Energy Outlook 2022.” [Online]. Available: [www.iea.org/t&c/](http://www.iea.org/t&c/)
- [4] D. T. Ton and M. A. Smith, “The U.S. Department of Energy’s Microgrid Initiative,” *Electricity Journal*, vol. 25, no. 8, pp. 84–94, 2012, doi: 10.1016/j.tej.2012.09.013.
- [5] F. Delfino, R. Procopio, M. Rossi, S. Bracco, M. Brignone, and M. Robba, “Microgrid Design and Operation Toward Smart Energy in Cities.”, Italy, Complete Edition, Aug. 2018.
- [6] G. Chicco, “01RUKND Smart electricity systems Course Notes”, Politecnico di Torino, Italy, 2023.
- [7] A. C. Z. de Souza, B. De Nadai, F. M. Portelinha, D. Marujo, and D. Q. Oliveira, “Microgrids operation in islanded mode,” *Sustainable Development in Energy Systems*, pp. 193–215, Sep. 2017, doi: 10.1007/978-3-319-54808-1\_10/COVER.
- [8] M. H. Saeed, W. Fangzong, B. A. Kalwar, and S. Iqbal, “A Review on Microgrids’ Challenges Perspectives,” *IEEE Access*, vol. 9. Institute of Electrical and Electronics Engineers Inc., pp. 166502–166517, 2021. doi: 10.1109/ACCESS.2021.3135083.
- [9] “IEA, Annual grid-scale battery storage additions, 2017-2022, IEA, Paris <https://www.iea.org/data-and-statistics/charts/annual-grid-scale-battery-storage-additions-2017-2022>, IEA. Licence: CC BY 4.0.”
- [10] “Energy storage - IEA.” Available: <https://www.iea.org/energy-system/electricity/grid-scale-storage>
- [11] Janaka Ekanayake, Kithsiri Liyanage, Jianzhong Wu, Akihiko Yokoyama, and Nick Jenkins, “Smart Grid Technology and Applications”, United Kingdom, 2012 Edition.
- [12] E. Chiavazzo, “01TVHND Energy storage Course Notes”, Politecnico di Torino, Italy, 2023.
- [13] M. Santarelli, “01QGXND Polygeneration and advanced energy systems”, Politecnico di Torino, Italy, 2023.
- [14] “Battery Energy Storage Systems (BESS) | What It Is & How It Works.” [Online]. Available: <https://www.carboncollective.co/sustainable-investing/battery-energy-storage-systems-bess>
- [15] “Battery Energy Storage System (BESS) | The Ultimate Guide.” [Online]. Available: <https://www.edina.eu/power/battery-energy-storage-system-bess>
- [16] “Critical Minerals – Topics - IEA.” [Online]. Available: <https://www.iea.org/topics/critical-minerals>
- [17] “Lithium - Price - Chart - Historical Data - News.” Accessed: Jan. 14, 2024. [Online]. Available: <https://tradingeconomics.com/commodity/lithium>

- [18] Loccioni, "EPC Contractor Documentation," 2023.
- [19] E.ON, "Customer Documentation," 2023.
- [20] "Power System Solutions - DigSILENT." Accessed: Available: <https://www.digsilent.de/en/>
- [21] DigSILENT GmbH, *DigSILENT PowerFactory User Manual - Version 2023*.
- [22] DigSILENT GmbH, "PowerFactory Technical Reference: Static Generator. "
- [23] "What is neutral earth compensator? - Answers." Available: [https://www.answers.com/Q/What\\_is\\_neutral\\_earth\\_compensator](https://www.answers.com/Q/What_is_neutral_earth_compensator)
- [24] "WHAT IS A NEUTRAL EARTHING RESISTOR?" [Online]. Available: <https://ampcontrolgroup.com/news/what-neutral-earthing-resistor>
- [25] DigSILENT GmbH, "PowerFactory Technical Reference: Overhead Line Models".
- [26] Anie Energia, "Energy Efficiency Ecodesign for transformers." Italy, 2015
- [27] O. A. Afolabi, W. H. Ali, P. Cofie, J. Fuller, P. Obiomon, and E. S. Kolawole, "Analysis of the Load Flow Problem in Power System Planning Studies," *Energy Power Eng*, vol. 07, no. 10, pp. 509–523, 2015, doi: 10.4236/epe.2015.710048.
- [28] "Newton Raphson Method for Load Flow Analysis." [Online]. Available: <https://www.eeeguide.com/newton-raphson-method-for-load-flow-analysis/>
- [29] DigSILENT GmbH, "INTRODUCTORY COURSE: LOAD FLOW AND SHORT CIRCUIT CALCULATION".
- [30] E. Muljadi and V. Gevorgian, "Short-Circuit Modeling of a Wind Power Plant Preprint Short-Circuit Modeling of a Wind Power Plant," 2011. [Online]. Available: <http://www.osti.gov/bridge>
- [31] "AGN 168 ISSUE B/1/4 Application Guidance Notes: Technical Information from Cummins Generator Technologies AGN 168-Short Circuit Ratio (X/R)."

# Ringraziamenti

Innanzitutto, desidero ringraziare tutte le persone che mi hanno aiutato e fornito gli strumenti necessari per portare a termine questa tesi.

Un ringraziamento particolare va ai miei genitori per la fiducia che mi hanno dimostrato. Il loro sostegno è stato fondamentale per me.

Voglio ringraziare di cuore mia sorella Michela per essermi sempre stata vicina.

Infine, voglio ringraziare tutti i miei parenti e amici che mi hanno sostenuto durante il mio percorso universitario.